Journal of Medicinal Chemistry

Article

pubs.acs.org/jmc

Structure–Activity Relationships of Privileged Structures Lead to the Discovery of Novel Biased Ligands at the Dopamine D_2 Receptor

Monika Szabo,[†,‡] Carmen Klein Herenbrink,[‡] Arthur Christopoulos,[‡] J. Robert Lane,*[,‡] and Ben Capuano*[,†]

[†]Medicinal Chemistry and [‡]Drug Discovery Biology, Monash Institute of Pharmaceutical Sciences, Monash University, Parkville 3052, Victoria, Australia

Supporting Information

ABSTRACT: Biased agonism at GPCRs highlights the potential for the discovery and design of pathway-selective ligands and may confer therapeutic advantages to ligands targeting the dopamine D_2 receptor (D_2R). We investigated the determinants of efficacy, affinity, and bias for three privileged structures for the D_2R, exploring changes to linker length and incorporation of a heterocyclic unit. Profiling the compounds in two signaling assays (cAMP and pERK1/2) allowed us to identify and quantify determinants of biased agonism at the D_2R. Substitution on the phenylpiperazine privileged structures (2-methoxy vs 2,3-dichloro) influenced bias when the thienopyridine heterocycle was absent. Upon inclusion of the thienopyridine unit, the substitution pattern (4,6-dimethyl vs 5-chloro-6-methoxy-4-methyl) had a significant effect on bias that overruled the effect of the phenylpiperazine substitution pattern. This latter observation could be reconciled with an extended binding mode for these compounds, whereby the interaction of the heterocycle with a secondary binding pocket may engender bias.

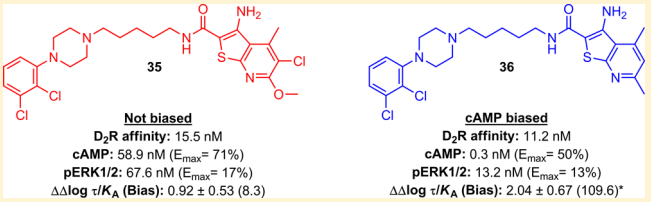

INTRODUCTION

Dopamine receptors (DRs) belong to the G-protein-coupled receptor (GPCR) superfamily that is characterized by seven transmembrane (TM) domains. There are five receptor subtypes (D_1–D_5) expressed both in the central nervous system (CNS) and in the periphery.[1] In the CNS the dopamine D_2 receptor (D_2R) is a primary target for the treatment of disease including Parkinson's and schizophrenia.[2] Antipsychotics have evolved from first generation antipsychotics (FGAs), which act as D_2 antagonists, to second generation antipsychotics (SGAs), which display robust polypharmacology with high affinities for GPCRs in addition to the D_2R.[3−5] Aripiprazole (**1**, Figure 1) is classified as a third generation antipsychotic (TGA). This comes from its unique pharmacological profile, as it is a potent partial agonist at both presynaptic and postsynaptic D_2 receptors while also displaying partial agonist activity at the serotonin 5-HT_{1A} receptor.[6−8] The exploration of D_2R partial agonists for treating schizophrenia was driven by the hypothesis that they would stabilize levels of dopamine in the CNS but avoid the extrapyramidal side effects associated with complete D_2R blockade (for a detailed review of the use of partial agonists in the treatment of schizophrenia and other related psychoactive disorders, see Tamminga et al.[9]). Since the discovery of aripiprazole, other partial agonists have emerged, such as cariprazine (**2**), brexpiprazole (**3**), and bifeprunox (**4**) (Figure 1), with **2** currently awaiting FDA approval and **3** in phase III clinical trials for the treatment of schizophrenia.

Biased agonism (sometimes termed "functional selectivity" or "stimulus bias") refers to the phenomenon by which different agonists acting at the same receptor can stabilize distinct receptor conformations linked to different functional responses.[10−12] Of interest, aripiprazole has been identified as a ligand that displays biased agonism, and evidence has been provided that this bias may contribute to its antipsychotic efficacy.[13] Previous SAR studies, focused on aripiprazole, revealed that small structural changes to the phenylpiperazine core, the linker region, and the bicyclic heterocycle resulted in changes in biased agonism. These studies identified novel D_2R ligands that displayed bias toward the recruitment of β-arrestin.[14,15] Further examples of biased agonists targeting the D_2R have been provided by a number of groups, including Mailman et al. with dihydrexidine,[16,17] Tschammer et al. with 1,4-disubstituted phenylpiperazines,[18] and Shonberg et al. with tetrahydroisoquinoline derivatives.[19]

Privileged structures are often versatile scaffolds that can be functionalized to produce ligands that may be selective for a class of receptors and, more ideally, a single receptor target.[20−23] Privileged structures can be "built in" to a molecule by replacing certain functional groups or can be used as the starting scaffold, where one can "build out" to create an optimized ligand. The aim of the current study was to investigate the structure–activity relationships underlying affinity and efficacy of distinct privileged structures for the

Received: March 24, 2014

dx.doi.org/10.1021/jm500457x | J. Med. Chem. XXXX, XXX, XXX–XXX

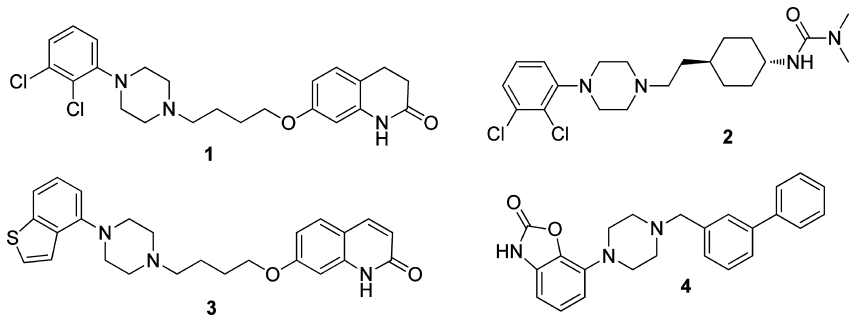

Figure 1. Partial agonists: aripiprazole (**1**), cariprazine (**2**), brexpiprazole (**3**), and bifeprunox (**4**).

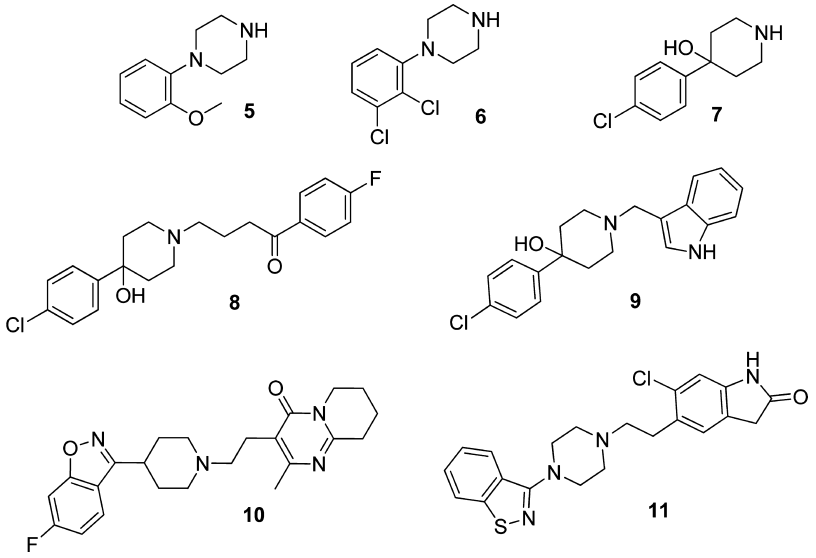

Figure 2. Privileged structures: 2-methoxyphenylpiperazine (**5**), 2,3-dichlorophenylpiperazine (**6**), and 4,4-chlorophenyl-4-hydroxypiperidine (**7**). Antipsychotics and/or potent D_2R antagonists: haloperidol (**8**), L-741,626 (**9**), risperidone (**10**), and ziprasidone (**11**).

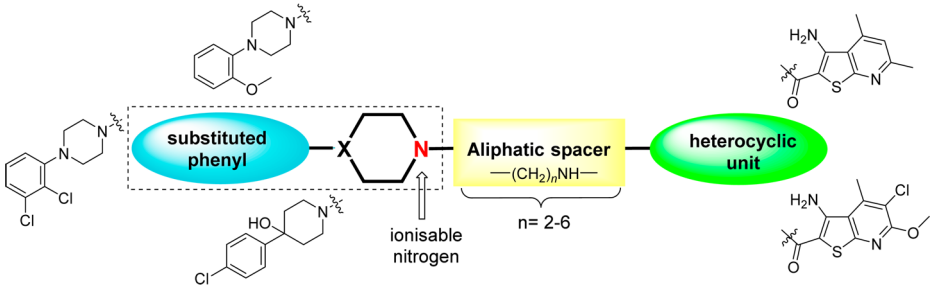

Figure 3. Model pharmacophore for the development of novel D_2R antagonists and/or partial agonists.

D_2R. Many ligands targeting the D_2R incorporate a substituted phenylpiperazine; therefore, we selected 2-methoxyphenylpiperazine (**5**) and 2,3-dichlorophenylpiperazine (**6**) to use as privileged structures in our study (Figure 2). We also investigated 4,4-chlorophenyl-4-hydroxypiperidine (**7**), as it represents a common structural feature of two very potent D_2 antagonists, haloperidol (**8**) and L-741,626 (**9**)[24] (Figure 2). Another structural attribute of many D_2R targeting antagonists and partial agonists is the incorporation of a linker to the ionizable nitrogen, usually from two to five atoms in length followed by a heterocyclic group. For example, the two antipsychotics risperidone (**10**) and ziprasidone (**11**), while devoid of a substituted phenylpiperazine moiety, retain either a piperazine or a piperidine system to bear the ionizable nitrogen, a spacer, and a heterobicyclic group (Figure 2). Such scaffolds have been shown to confer subtype selectivity across the D_2-like receptor subfamily.[25] However, of relevance to this study, Newman and co-workers revealed that the presence of a heterocyclic group, or even the linker alone, could modulate the efficacy of compounds based on **6** in an assay measuring activation of a $G\alpha_{o1}$ G protein. In contrast, an equivalent compound based on **5** displayed no agonism at this assay end point.[26] These observations beg the question whether such structural determinants of efficacy are consistent across different signaling end points or whether they differ and thus engender biased agonism.

In our study, we have synthesized and characterized a focused library of novel D_2R antagonists and partial agonists based on a previously described structural model[27] (Figure 3) incorporating the aforementioned three privileged structures,

dx.doi.org/10.1021/jm500457x | J. Med. Chem. XXXX, XXX, XXX−XXX

Scheme 1. Synthesis of Various Linker Lengths Incorporating Privileged Structures[a]

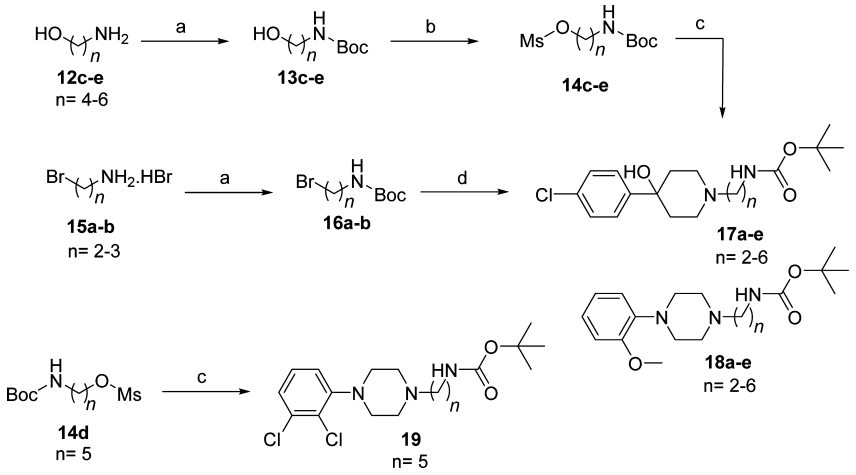

[a]Reagents and conditions: (a) Boc anhydride, Et_3N, DCM, rt, 1−1.5 h, 28−96%; (b) methanesulfonyl chloride, Et_3N, DCM, 0 °C → rt; (c) **5**, **6**, or **7**, CH_3CN, reflux, 24 h, 28−64%; (d) **5** or **7**, NaI, DIPEA, CH_3CN, reflux, 24 h, 34−93%.

Scheme 2. Synthesis of Key Thienopyridine Scaffolds[a]

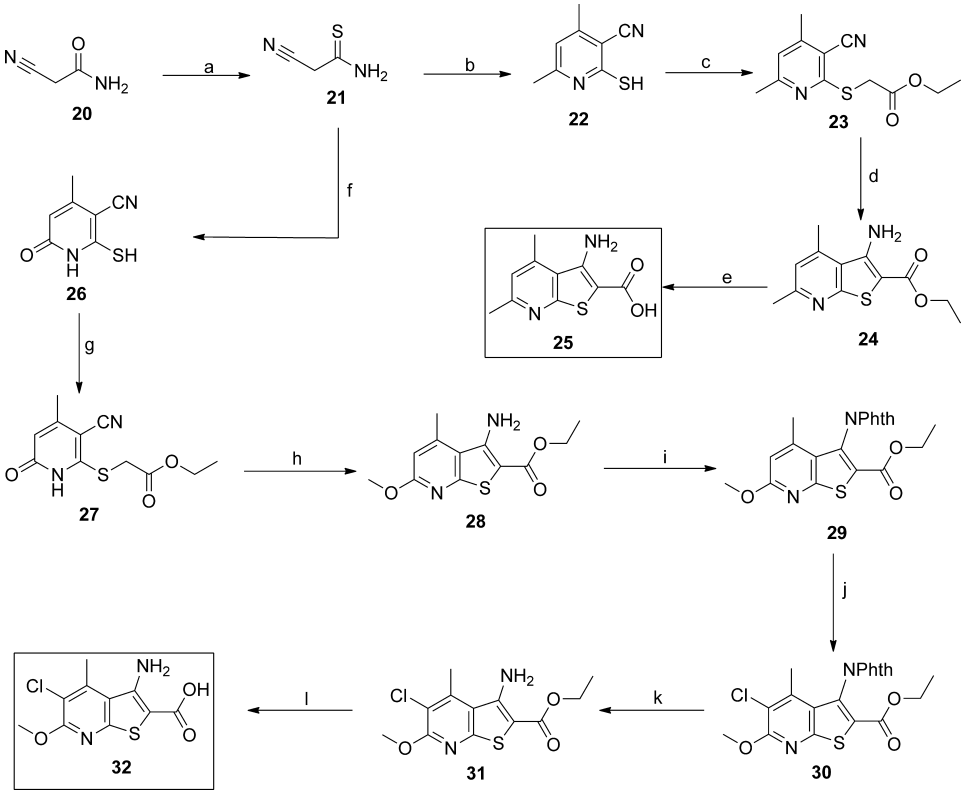

[a]Reagents and conditions: (a) P_4S_{10}, EtOAc, reflux 1.5−4 h, 30%; (b) acetylacetone, KOH, MeOH, reflux, 4 h, 67%; (c) ethyl 2-chloroacetate, Et_3N, 0 °C → rt, 3.5 h, 86%; (d) 1 M KOH, DMF, rt, 15 min, 93%; (e) 2 M NaOH, EtOH, reflux, 4 h, 83%; (f) methyl acetoacetate, morpholine, EtOH, reflux 8 h, 51%; (g) ethyl 2-chloroacetate, Et_3N, DMF, 0 °C → rt, 5 h, 81%; (h) (i) MeI, K_2CO_3, DMF, 4 h, rt; (ii) 1 M KOH, 15 min, 58%; (i) phthalic anhydride, AcOH, reflux, 20 h, 55%; (j) *N*-chlorosuccinimide, conc HCl, EtOH, reflux, 1.5 h, 93%; (k) $(NH_2)_2{\cdot}H_2O$, EtOH, reflux, 3 h, 84%; (l) 2 M NaOH, EtOH, reflux, 1.5 h, 84%.

different spacer lengths (ranging from two to six carbon atoms), and novel heterocyclic units identified from our in-house muscarinic GPCR drug discovery program. These versatile heterocyclic motifs were selected, as they exhibit structural similarities to that of the tetrahydroquinolinone moiety of aripiprazole. Additionally, the use of a thiophene has previously been shown to be advantageous in increasing the affinity for D_2-like receptor subtypes, relating to its electron-rich system and its ability to form hydrophobic interactions within a binding pocket, essentially acting as an isostere of benzene.[28] As such, we envisioned that our thienopyridine scaffolds may also exhibit these properties. The ligands generated were evaluated using in vitro assays to measure their ability to displace [^{3}H]spiperone binding at the D_2R and to stimulate ERK1/2 phosphorylation

dx.doi.org/10.1021/jm500457x | J. Med. Chem. XXXX, XXX, XXX−XXX

through activation of the D_2R. For selected compounds, we extended our characterization to a second functional assay, inhibition of forskolin-induced cAMP production, to allow identification and quantification of biased agonism.[29]

RESULTS AND DISCUSSION

Chemistry. Derivatives of the previously described privileged structures (**5**–**7**) were synthesized utilizing a single linkage point, namely, the aliphatic nitrogen of the piperazine or piperidine, and included chain lengths of two to six carbon atoms (Scheme 1). To furnish derivatives with linker lengths of two to three carbon atoms, we commenced with bromoalkanamines (**15a,b**) and subsequently Boc-protected the amines to afford the intermediates **16a,b**. These compounds were then reacted with **5** or **7** to give products **17a,b** and **18a,b** in yields ranging from 34% to 93%. We utilized a modified pathway for generating the required analogues **17c**–**e** and **18c**–**e**, since linker lengths greater than four carbon atoms were not directly available as the bromoalkanamines. Aminoalkanols (**12c**–**e**) with carbon atom spacers of four to six were Boc-protected to give intermediates **13c**–**e** in excellent yields (83–96%). The primary alcohol functionality was activated with methanesulfonyl chloride to generate the mesylated intermediates **14c**–**e**. Because of the reactivity and/or stability of the mesylated compounds, the formation of products was confirmed by the disappearance of starting material via TLC and then reacted immediately without further purification in the next reaction. Subsequent reaction of **5** or **7** with the mesylates **14c**–**e** produced analogues **17c**–**e** and **18c**–**e**. To furnish the five carbon atom spaced Boc protected 2,3-dichlorophenylpiperazine (**19**), the mesylate **14d** was reacted with **6** under the same conditions as described above.

Synthesis of the thienopyridine scaffold is represented in Scheme 2 and commences with reacting 2-cyanoacetamide (**20**) with phosphorus pentasulfide (P_4S_{10}) to afford 2-cyanothioacetamide (**21**) in approximately 30% after recrystallization. To synthesize the 4,6-dimethylthienopyridine compound, **21** was reacted with acetylacetone under basic conditions to form the 4,6-dimethyl substituted pyridine core (**22**) in 67% yield. Subsequent reaction of **22** with ethyl 2-chloroacetate under basic conditions gave the monocyclic ethyl ester (**23**). The monocyclic structure was successfully converted to the bicyclic form (**24**) in rapid time (15 min) in the presence of 1 M aqueous potassium hydroxide. Ester hydrolysis of **24** using 2 M sodium hydroxide in ethanol, followed by acidic workup, gave the first key thienopyridine core carboxylic acid (**25**). To furnish the 5-chloro-6-methoxy-4-methylthienopyridine scaffold, compound **21** was reacted with methyl acetoacetate and morpholine which initially afforded the product as the morpholinium salt. The desired thiol (**26**) was isolated in the free form by acidification with 1 M aqueous hydrochloric acid. Further reaction with ethyl chloroacetate gave the monocyclic ethyl ester (**27**) in good yield (81%). In order to convert the pyridinone into the corresponding pyridine alkyl ether, **27** was reacted with iodomethane under basic conditions. One equivalent of a stronger base, such as 1 M aqueous potassium hydroxide, was necessary to ensure complete conversion to the thienopyridine scaffold (**28**). It was imperative to protect the free amine of the bicycle prior to chlorination at the 5′ position to avoid N-halogenation. Phthalic anhydride was employed under acidic conditions which resulted in the phthalimide-protected product (**29**) in good yield. *N*-Chlorosuccinimide (NCS) was used to install the chlorine atom at the 5′ position to give **30** in excellent yield. Subsequent removal of the phthalimide protecting group using hydrazine monohydrate afforded **31** in excellent yield. Finally, the base-catalyzed ester hydrolysis conditions mentioned earlier were commissioned that, following acidic workup, afforded the key carboxylic acid intermediate compound, **32**.

The syntheses of the target compounds incorporating privileged structures **5**, **6**, and **7** and the thienopyridine scaffolds are summarized in Scheme 3. We initially combined

Scheme 3. Synthesis of Full Length Structures Including Privileged Structures, Linker, and Thienopyridine Scaffold[a]

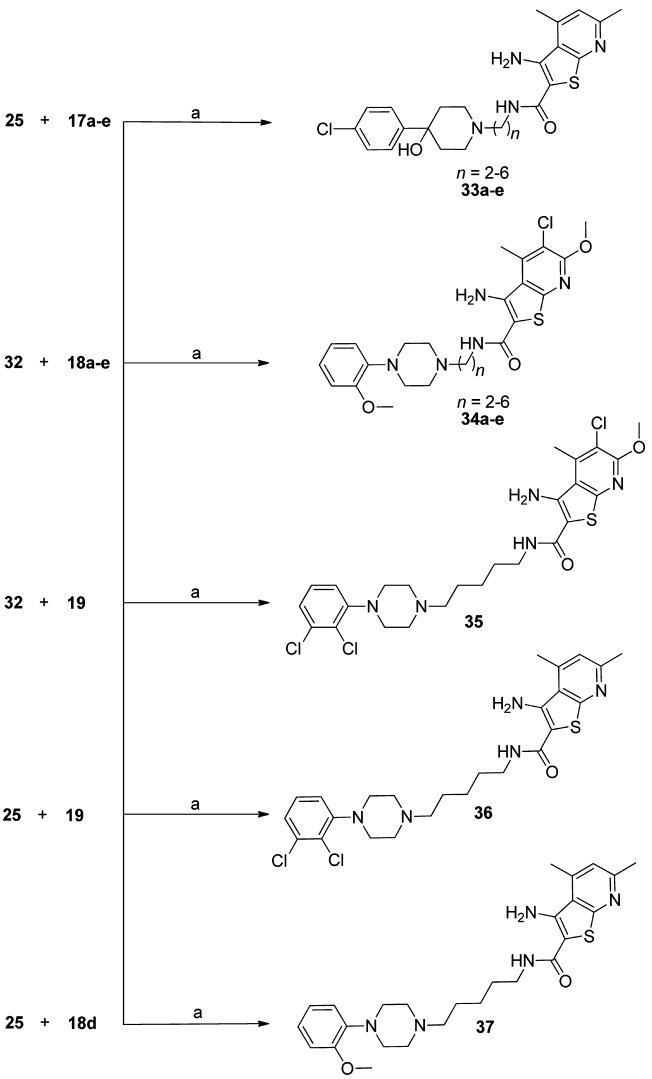

[a]Reagents and conditions: Compounds **17a**–**e**, **18a**–**e**, and **19** were all deprotected prior to performing the coupling reaction. (a) BOP reagent, DIPEA, DMF, rt, 1–12 h, 29–70%.

the 4,4-chlorophenyl-4-hydroxypiperidine analogues (**17a**–**e**), which were deprotected prior to use, with the 4,6-dimethylthienopyridinecarboxylic acid (**25**). This was carried out using a BOP-mediated coupling reaction to give analogues **33a**–**e** in 31–56% yield. Similarly the 2-methoxyphenylpiperazine analogues **18a**–**e** following Boc deprotection were coupled to the carboxylic acid **32** to furnish the target compounds **34a**–**e** in respectable yield. Compound **19**, following removal of the protecting group, was then

dx.doi.org/10.1021/jm500457x | J. Med. Chem. XXXX, XXX, XXX–XXX

immediately reacted with **32** to yield the analogue **35**, while compound **25** furnished analogue **36**. Reaction of the carboxylic acid precursor **25** with **18d** (Boc deprotected) in the presence of BOP also afforded compound **37** in respectable yield.

Pharmacology. *Binding Characterization of Privileged Structures and Linkers.* Both **5** and **6** privileged structures have been evaluated in terms of their ability to bind the D_2R in a previous study.[26] We therefore evaluated the binding affinities of **7**, incorporating linker lengths of two to six carbon atoms and conserving the Boc group for stability purposes and to add lipophilicity to the end of the linker, with equivalent **5** structures as comparators. As expected, both privileged structures (**5** and **7**) demonstrated poor binding affinity (~10 μM, Table 1), most likely because of their small fragment-like

Table 1. Binding Data at the Dopamine D_2R for 2-Methoxyphenylpiperazine and 4,4-Chlorophenyl-4-hydroxypiperidine Linker Derivatives[a]

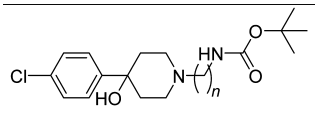

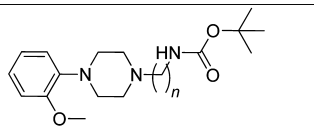

Compound	*n*	pK_i ± SEM (K_i, nM)	Compound	*n*	pK_i ± SEM (K_i, nM)
7	-	5.04 ± 0.13 (9090)	**5**	-	5.39 ± 0.08 (4110)
17a	2	5.56 ± 0.08 (2750)	**18a**	2	6.77 ± 0.17 (171)
17b	3	5.87 ± 0.07 (1350)	**18b**	3	7.80 ± 0.27 (16.1)
17c	4	5.68 ± 0.06 (2110)	**18c**	4	7.72 ± 0.17 (18.9)
17d	5	5.69 ± 0.05 (2050)	**18d**	5	7.92 ± 0.24 (12.1)
17e	6	6.05 ± 0.06 (902)	**18e**	6	7.13 ± 0.05 (74.8)

[a]Compounds were tested against [^{3}H]spiperone through competition binding studies using D_{2L} CHO cell membranes. Data represent the mean ± SEM of three separate experiments performed in duplicate.

size that confers minimal points for contact with residues in the D_2R orthosteric pocket. Modest increases in affinity were observed upon addition of the linkers to **7** (**17a**–**e**) with the six carbon atom linker (**17e**) conferring a 10-fold increase in affinity. Comparatively, a more pronounced increase in binding affinity was evident for the 2-methoxyphenylpiperazine derivatives (Table 1). Analogues containing a three, four, or five carbon atom linker (**18b**–**d**) demonstrated enhanced affinity compared to the two carbon atom linker (**18a**), with these analogues displaying a 200-fold increase in affinity compared to **5** alone. However, there seems to be no clear linker length dependence for affinity within this set of compounds **18b**–**e** (n = 3–6).

Binding Characterization of Full-Length Structures. We then investigated the effect of the addition of a heterocyclic group to each of the linkers as indicated in our model pharmacophore (Figure 3). While the substitution pattern on each of the heterocycles listed in Table 2 is different (4,6-dimethyl vs 5-chloro-6-methoxy-4-methyl), the general core of the heterocycle (thienopyridine) is the same. The subtle differences in these substitutions and their consequences on pharmacology at the D_2R will be explored at a later stage in our SAR study. The results in Table 2 showed that analogues based on privileged structure **7** (**33a**–**e**) bind the D_2R with only moderate affinity (micromolar range) with no significant increase compared to the equivalent linker precursors (Table

Table 2. Binding Data at the Dopamine D_2R for 2-Methoxyphenylpiperazine and 4,4-Chlorophenyl-4-hydroxypiperidine Full Length Derivatives[a]

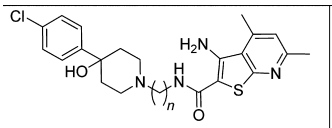

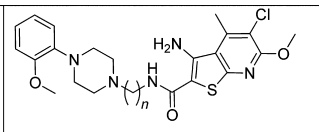

Compound	*n*	pK_i ± SEM (K_i, nM)	Compound	*n*	pK_i ± SEM (K_i, nM)
33a	2	6.04 ± 0.10 (910)	**34a**	2	7.32 ± 0.07 (48.3)
33b	3	5.77 ± 0.12 (1700)	**34b**	3	7.71 ± 0.18 (19.5)
33c	4	5.65 ± 0.08 (2250)	**34c**	4	8.20 ± 0.15 (6.3)
33d	5	5.70 ± 0.07 (1980)	**34d**	5	8.45 ± 0.06 (3.5)
33e	6	6.01 ± 0.04 (975)	**34e**	6	9.21 ± 0.03 (0.6)

[a]Compounds are tested against [^{3}H]spiperone through competition binding studies using D_{2L} CHO cell membranes. Data represent the mean ± SEM of three separate experiments performed in duplicate.

1). A similar analogue using privileged structure **7** in combination with the heterocycle present in aripiprazole (dihydroquinolinone) showed poor binding affinity at the D_2R;[30] therefore, this is consistent with our results. Structures incorporating **5** retained their affinity, and in the cases of the two and six carbon atom spacers (**34a** and **34e**), their binding affinities were improved in comparison to their linker precursors (**18a** and **18e**). On this occasion, a definite trend of increasing binding affinity with carbon linker length was evident, with the six carbon atom linker derivative (**34e**) as the standout displaying subnanomolar affinity (K_i = 0.6 nM). This notable enhancement in affinity is supported by literature that describes a secondary hydrophobic pocket in the D_2R that is only reached via longer chain lengths. Interaction with this secondary pocket has been demonstrated to confer both increases in affinity and subtype selectivity.[18,26,31] While we acknowledge that the heterocycles added to these two distinct privileged structures are subtly different, the lack of affinity gain observed for the 4,6-dimethyl substituted thienopyridine derivatives (**33a**–**e**) is unlikely to be attributed to this difference.

SAR of 2-Methoxyphenylpiperazine Linkers and Full Structures: ERK1/2 Phosphorylation Assays. To expand on our initial results with the **5** and **7** series linkers and full structures (Tables 1 and 2), we tested these compounds in functional ERK1/2 phosphorylation (pERK1/2) assays. Analogues **5**, **7**, **17a**–**e**, **18a**–**e**, **33a**–**c**, and **34a**–**e** at 10 μM were initially tested in time-course assays to identify potential agonists and determine the appropriate peak stimulation time for subsequent construction of concentration–response curves. Compounds derived from **7** displayed no agonism (data not shown). As such, while also considering their poor binding affinities, we did not pursue these compounds for further characterization. Ligands **5**, **18a**, and **18e** were determined to be antagonists (based on time-course data and binding data). They were further analyzed in a pERK1/2 assay for their ability to antagonize a 10 nM concentration of dopamine, to obtain values of inhibitory potency (pIC_{50}) for both compounds. We observed a striking increase in inhibitory potency from the parent molecule **5** (>1000 nM) to compounds containing a linker (**18a**, 93.3 nM; **18e**, 3.98 nM). The remainder of compounds displayed agonism in our time-course experiments (**18b**–**d**). These analogues exhibited partial agonism, consistent with the observations of Newman et al. using similar linked

dx.doi.org/10.1021/jm500457x | J. Med. Chem. XXXX, XXX, XXX–XXX

Table 3. Functional ERK1/2 Phosphorylation Assays at the Dopamine D_2 Receptor for 2-Methoxyphenylpiperazine Linker Derivatives[a]

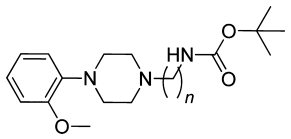

compd	*n*	pIC_{50} ± SEM (IC_{50}, nM)[b]	pEC_{50} ± SEM (EC_{50}, nM)[c]	E_{max} ± SEM (% DA)[d]
5	na	<6 (>1000)		
18a	2	7.03 ± 0.54 (93.3)		
18b	3		9.41 ± 0.15 (0.39)	31 ± 1
18c	4		9.22 ± 0.25 (0.60)	13 ± 1
18d	5		8.84 ± 0.16 (1.43)	19 ± 1
18e	6	8.40 ± 0.29 (3.98)		

[a]Data represent the mean ± SEM of three to four separate experiments performed in duplicate. [b]Values are obtained via interacting ligands with a 10 nM concentration of dopamine. [c]Values are obtained via concentration−response assays at the appropriate stimulation time. [d]E_{max} data are represented as a % of the maximal effect of dopamine (DA).

Table 4. Functional ERK1/2 Phosphorylation Assays at the Dopamine D_2R for Compounds Containing the 2-Methoxyphenylpiperazine Privileged Structure[a]

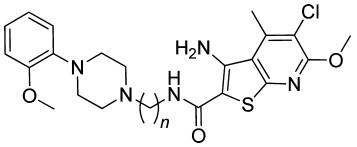

compd	*n*	pK_B ± SEM (K_B, nM)[b]	pEC_{50} ± SEM (EC_{50}, nM)[c]	E_{max} ± SEM (% DA)[d]
5	na	6.32 ± 0.18 (479)		
34a	2	6.45 ± 0.17 (355)		
34b	3	6.13 ± 0.16 (741)		
34c	4	6.31 ± 0.14 (490)		
34d	5		8.57 ± 0.66 (2.69)	17 ± 4
34e	6		8.26 ± 0.31 (5.49)	14 ± 2

[a]Data are the mean of four to five experiments ± SEM. [b]Data are based on interaction studies with varying concentrations of dopamine. Data are fit to the Gaddum−Schild model of competitive antagonism using Graph Pad Prism (version 6) with Schild slopes constrained to 1. [c]Values are attained from concentration−response curves at the appropriate concentration and stimulation time. [d]E_{max} data are represented as a % of the maximal effect of dopamine (DA).

derivatives of **5**[26] (Table 3). The four-carbon atom spacer **18c** has a lower E_{max} (the maximum stimulation achieved as a percentage of the maximal effect of dopamine, E_{max} = 13 ± 1) compared to the five-carbon atom spacer **18d** (E_{max} = 19 ± 1). The three-carbon atom spacer analogue (**18b**) displayed a significantly higher E_{max} of 31 ± 1 ($P < 0.05$). An enhancement of affinity at the D_2R was observed for a similar series of compounds upon addition of alkyl linkers to **5**.[26] We also observed an enhancement of affinity (Table 1) consistent with the hypothesis of Newman et al. whereby this increase in affinity is conferred by additional hydrophobic interactions between residues within the orthosteric pocket of the D_2R and the linker. However, we also observe a gain in agonist efficacy that is dependent on linker length (Table 3). This pattern is distinct from the lack of effect of the addition of a linker to the scaffold of **5** observed by Newman et al. This discrepancy could be due to the subtle differences between the two sets of compounds, the different cell backgrounds used in these experiments, or the different assay end point used to measure agonism (pERK1/2 of our study vs $G\alpha_{o1}$ G protein coupling of Newman et al).

Next we investigated if such linker length dependencies in efficacy are also observed for those compounds with a heterocyclic group attached to the linker. Table 4 represents the functional data for compounds **34a−e** at the D_2R. We identified compounds **34a−c** (linker lengths from two to four carbon atoms) as antagonists and compounds **34d−e** (with linker lengths of five and six carbon atoms, respectively) as partial agonists. This pattern is distinct from the linker only compounds (**18a−e**) in which a linker length of three carbon atoms was optimal in terms of the maximal effect of the agonist. The partial agonists **34d** and **34e** displayed the same maximum response at the D_2R (E_{max}= 17 ± 4 and 14 ± 2, respectively). Moreover, the partial agonism observed in the five carbon atom 2-methoxyphenylpiperazine linker (**18d**, E_{max} = 19 ± 1) was maintained upon incorporation of the heterocyclic group to the linker (**34d**, E_{max} = 17 ± 4). Compounds **34a−c** displayed no gain in functional affinity (pK_B) compared to the parent molecule **5**.

In combination, these data highlight that subtle changes to the linker length appear to be important in switching between antagonism and partial agonism. Of note, the pattern is different for linker analogues as opposed to the extended structures with a heterocycle group suggesting a different binding mode at the D_2R.

Biased Agonism at the D_2R. The partial agonists **34d** and **34e** displayed similar binding affinity (Table 2) and functional activity (Table 4). The 2,3-dichlorophenylpiperazine moiety

dx.doi.org/10.1021/jm500457x | J. Med. Chem. XXXX, XXX, XXX−XXX

Table 5. Binding Data for Compounds at the D_2R That Incorporate 2,3-Dichlorophenylpiperazine and Have Variations to the Thienopyridine Unit[a]

Compound	Structure	$pK_i \pm SEM$ (K_i, nM)[b]
6	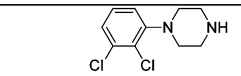	5.94 ± 0.05 (1160)
19	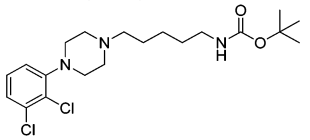	7.37 ± 0.08 (42.6)
35	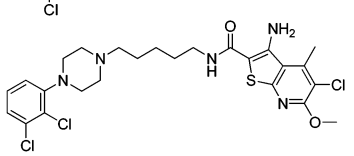	7.81 ± 0.11 (15.5)
36	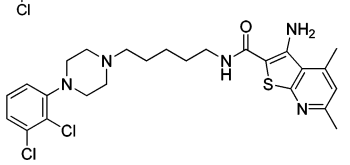	7.95 ± 0.06 (11.2)
37	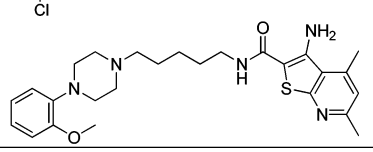	8.04 ± 0.03 (9.1)

[a]Compounds are tested using [^{3}H]spiperone through competition binding studies using D_{2L} CHO cell membranes. [b]Data represent the mean ± SEM of three separate experiments performed in duplicate.

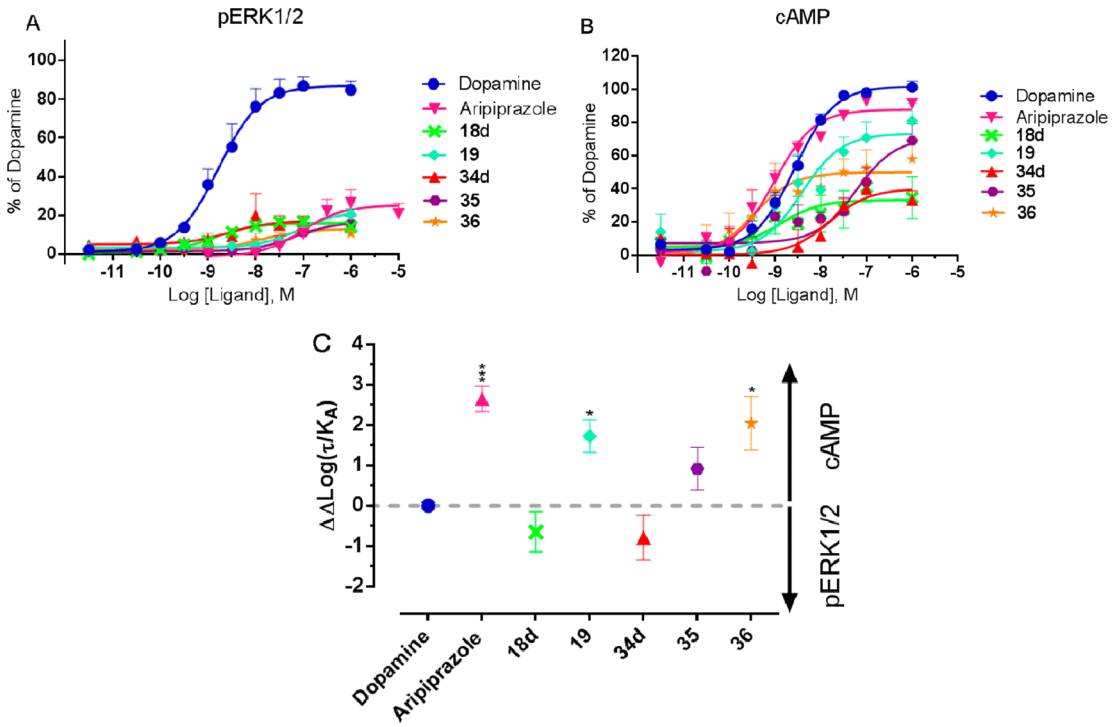

Figure 4. (A) ERK1/2 phosphorylation concentration−response assays. (B) Inhibition of FSK-induced cAMP production. (C) Bias plot representing the bias factor ($\Delta\Delta\log(\tau/K_A)$) of ligands between pERK1/2 and cAMP signaling pathways. Values are represented in Table 6

and the aromatic bicycle of aripiprazole are separated by a five-atom spacer. This is analogous to the five carbon atom spacer separating the substituted thienopyridine and the 2-methoxyphenylpiperazine motif of compound **34d**. Therefore, we decided to further investigate **34d** based upon its linker length and structural similarity to aripiprazole. In particular, given that a number of studies have described aripiprazole as a biased agonist,[8,13] we extended our characterization of a limited number of compounds to activity at two assay end points, ERK1/2 phosphorylation and inhibition of forskolin stimulated cAMP production. In order to gain some preliminary SAR around this compound, we synthesized a small number of compounds related to **34d**. We retained the five-carbon atom linker for all derivatives and instead focused on subtle structural

dx.doi.org/10.1021/jm500457x | J. Med. Chem. XXXX, XXX, XXX−XXX

Table 6. Calculated Bias Factors and Functional Affinities for Selected Full Agonists and Partial Agonists at the Dopamine D_{2L} Receptor

		Inhibition of FSK-induced cAMP production[a]				ERK1/2 phosphorylation[a]				
Agonist	Structure	pK_A	logτ	Log τ/K_A	Δlog τ/K_A	pK_A	logτ	Log τ/K_A	Δlog τ/K_A	$\Delta\Delta$log τ/K_A (Bias)[b]
Dopamine	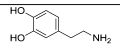	-	-	8.56 ± 0.07	0.00 ± 0.10	7.98 ± 0.18	0.79 ± 0.15	8.72 ± 0.05	0.00 ± 0.05	0.00 ± 0.09
Aripiprazole	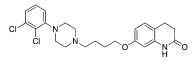	8.05 ± 0.29	0.82 ± 0.25	8.88 ± 0.13	0.32 ± 0.15	6.84 ± 0.33	-0.43 ± 0.10	6.39 ± 0.29	-2.33 ± 0.29	2.65 ± 0.33 (446.7)***
18d	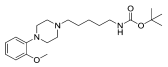	7.06 ± 0.27	0.19 ± 0.13	7.26± 0.21	-1.30 ± 0.22	8.77 ± 0.47	-0.67 ± 0.12	8.07 ± 0.45	-0.65 ± 0.45	-0.65 ± 0.50 (0.2)
19	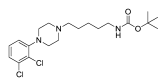	7.73 ± 0.26	0.43 ± 0.16	8.17 ± 0.16	-0.39 ± 0.17	7.14 ± 0.43	-0.51 ± 0.15	6.60 ± 0.37	-2.12 ± 0.37	1.73 ± 0.40 (53.7)*
34d	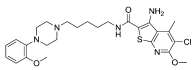	7.47 ± 0.43	-0.26 ± 0.18	7.23 ± 0.33	-1.33 ± 0.34	8.86 ± 0.48	-0.65 ± 0.13	8.18 ± 0.45	-0.54 ± 0.45	-0.79 ± 0.56 (0.2)
35	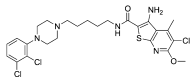	6.89 ± 0.32	0.28 ± 0.20	7.18 ± 0.18	-1.38 ± 0.19	7.10 ± 0.59	-0.65 ± 0.20	6.42± 0.50	-2.30 ± 0.50	0.92 ± 0.53 (8.3)
36	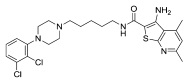	9.00 ± 0.29	-0.06 ± 0.11	8.96 ± 0.26	0.40 ± 0.27	7.90 ± 0.69	-0.78 ± 0.18	7.08 ± 0.62	-1.64 ± 0.62	2.04 ± 0.68 (109.6)*
37	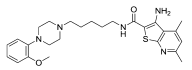	8.84 ± 0.39	-0.42 ± 0.13	8.45 ± 0.36	-0.11 ± 0.37	ND	ND	ND	ND	-

[a]Data are the mean of $n = 4$ experiments ± SEM. ND: no agonist activity detected. [b]Bias is defined as the fold bias relative to the reference agonist dopamine: (*) $P < 0.05$, (***) $P < 0.001$, significantly different from the reference agonist dopamine determined by a one-way ANOVA, Tukey post hoc test.

changes to the phenylpiperazine scaffold and the aromatic heterocyclic unit (thienopyridine scaffold). We utilized the 2,3-dichlorophenylpiperazine moiety present in aripiprazole and attached a five carbon atom spacer with the Boc appendage to generate ligand **19**. This compound was used as a comparator to compound **18d** which contains the same spacer but with the 2-methoxyphenylpiperazine moiety. We subsequently replaced the 2-methoxyphenylpiperazine moiety of **34d** with the 2,3-dichlorophenylpiperazine moiety to generate the target compound **35**. We also synthesized a further two analogues incorporating the simplified 4,6-dimethylthienopyridine to explore whether substitution around the thienopyridine core engendered an influence on bias. These structural motifs were combined with **6** and **5** to give **36** and **37**, respectively.

The new structures (**19** and **35**−**37**) were first tested in a binding assay to measure their biochemical affinity for the D_2R (Table 5). Compound **6** displayed a micromolar binding affinity for the D_2R similar to that of the other two privileged structures (**5** and **7**). A small but significant (3-fold) increase in affinity was observed upon addition of a heterocyclic unit (compounds **35** and **36**) to the linker derivative of **6**, compound **19** ($P < 0.05$). There is, however, no difference in the binding affinities of compounds **35**−**37**.

Given that the new set of analogues all exhibited noteworthy binding affinities (42.6−9.1 nM) for the D_2R, we extended our characterization to functional assays. Compounds **18d**, **19**, **34d**, **35**−**37**, the reference agonist dopamine, and control ligand aripiprazole were tested in pERK1/2 and cAMP (inhibition of forskolin-induced cAMP production) signaling pathways (Figure 4A and Figure 4B). We utilized a derivation of the operational model of agonism[32] to quantify bias by determining a transduction coefficient, log(τ/K_A), for all ligands at both pathways.[11] This transduction coefficient is a descriptor of the agonist effect of a single pathway that takes into account the intrinsic efficacy (τ) of the compound and its affinity (K_A) for the receptor coupled to that signaling pathway. The results from performing these analyses are summarized in Table 6 and displayed in Figure 4C. For values of potency (pEC_{50}) and maximal stimulation (E_{max}) for all compounds, see Supporting Information Table 1. We confirmed the biased action of aripiprazole, which displayed a 400-fold bias toward cAMP ($\Delta\Delta\log(\tau/K_A) = 2.65 \pm 0.32$) when compared to our reference agonist dopamine. Ligands **34d** and **35** both displayed no significant bias to either pathway; however, the linker derivative of **6** (**19**) showed a significant bias toward cAMP ($\Delta\Delta\log(\tau/K_A) = 1.73 \pm 0.40$). Conversely, the linker derivative of **5** (**18d**) did not display significantly different bias compared to dopamine. Compound **36** displayed biased agonism toward cAMP ($\Delta\Delta\log(\tau/K_A) = 2.04 \pm 0.67$), a bias profile that is statistically indistinguishable from that of aripiprazole and equates to a 100-fold bias toward the cAMP pathway. Compound **37** did not produce a response in pERK1/2 signaling assays but acted as a partial agonist in the cAMP assay. As such, we were unable to quantify the bias of this compound compared to dopamine. If we compare the transduction coefficient determined in the cAMP assay for **37** ($\log(\tau/K_A) = 8.45 \pm 0.36$) with those determined for **36** (changes in the phenyl substitution), **34d** (changes in the thienopyridine substitution pattern), and **18d** (no heterocyclic group), then compound **37** has a higher $\log(\tau/K_A)$ value in comparison to **34d** and **18d** and is similar to **36**. This means that compound **37** is at least as efficacious in the cAMP assay as compounds **34d**, **18d**, and **36** and suggests that compound **37** may also be a biased ligand. However, it is important to note that of all the

dx.doi.org/10.1021/jm500457x | J. Med. Chem. XXXX, XXX, XXX−XXX

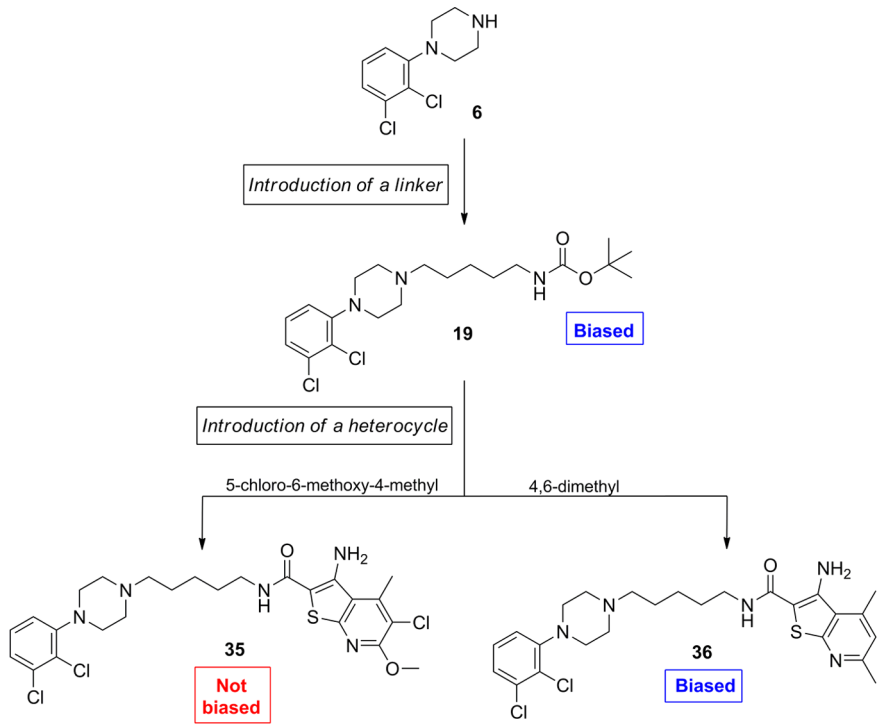

Figure 5. Progression of functionalizing privileged structure **6** with a linker (**19**) and substituted thienopyridine heterocycles (**35**, **36**).

compounds, **37** displays the lowest maximal effect (E_{max} = 33 ± 5) in the cAMP assay (Supporting Information Table 1). It is therefore possible that compound **37** is not a biased ligand relative to dopamine but that its action in the pERK1/2 assay was too weak to be detected.

Table 6 illustrates that the 2,3-dichlorophenylpiperazine derivative containing the *tert*-butylcarbamate five-carbon linker (**19**) is biased toward the cAMP pathway. Altering the substitution pattern on the phenyl ring from 2,3-dichloro to 2-methoxy gives compound **18d** that exhibits no bias for either the cAMP or pERK1/2 end points, thus highlighting that the substitution pattern on the phenylpiperazine moiety can itself confer differences in bias. Substitution around the phenyl ring on the phenylpiperazine moieties also seems to be important for bias for compounds that incorporate a tail heterocycle (**34d** versus **36**). Differences between 2-methoxyphenylpiperazine- and 2,3-dichlorophenylpiperazine-substituted analogues could be attributed to the electronic effects of these substituents, i.e., weakly inductively electron-withdrawing (-Cl) compared to moderately electron-donating (-OCH_3). Tschammer et al. also provided evidence that differential substitution of the phenyl moiety of phenylpiperazine ligands can modulate biased agonism at the D_2R.[18] Such observations are an extension of those made by Newman et al. whereby measuring G protein activation by the D_2R revealed that addition of linkers of different length and/or tail heterocyclic groups modulated agonist efficacy for derivatives of **6** whereas derivatives of **5** displayed no agonism.[26] However, replacing the 2-methoxyphenylpiperazine moiety on **34d** with **6** to give **35** does not produce significant biased agonism when compared to the reference agonist dopamine. If we simplify the thienopyridine core by altering the 5-chloro-6-methoxy-4-methyl substitution pattern with that of the 4,6-dimethyl substitution to give compound **36**, the biased agonism profile is recapitulated. This suggests that (1) the signaling pathway bias does not simply arise from the 2,3-dichlorophenylpiperazine moiety and (2) the substitution of the thienopyridine core has an important role in determining the bias profile of such compounds. The influence of the addition of a heterocycle upon both ligand affinity and efficacy suggests that this heterocycle makes an interaction with the D_2R. Newman et al. provided evidence of a secondary binding pocket that was exploited by extended phenylpiperazine ligands to gain subtype selectivity and modulate ligand efficacy.[26] It is tempting to speculate that our novel extended phenylpiperazine derivatives interact with an analogous secondary binding pocket and the nature of this interaction influences biased agonism.

Taking advantage of the partial agonism displayed by the compounds in this study, we were able to determine values of functional affinity (K_A) and efficacy (τ) as separate parameters rather than the composite transduction coefficient (log τ/K_A) (Table 6). By doing this, we can observe which of these parameters might be important drivers for signal bias at the D_2R. First, if we compare our partial agonists in Table 6, there are no significant differences between the ligands in terms of functional affinity (pK_A) in the pERK1/2 signaling pathway or efficacy (τ) at both pathways. However, in the cAMP signaling pathway, compound **36** exhibits a functional affinity that is significantly different from analogues **18d**, **34d**, and **35** ($P < 0.05$). As such, the distinct bias profile displayed by compound **36** is largely driven through a change in functional affinity at the cAMP assay. This is consistent with the findings of an SAR exploration of biased agonsim at the D_2R focused on cariprazine.[19] It is also of interest to compare the different parameters of compound **36** with that of aripiprazole. Both have very similar scaffolds and display a bias profile that is not statistically different. Although both have a similar transduction coefficient in the cAMP assay, compound **36** has a 10-fold higher functional affinity but a 10-fold lower efficacy at this pathway compared to aripiprazole. Similarly, in the pERK1/2 end point, compound **36** displays a 10-fold higher functional affinity than aripirazole but a smaller value of efficacy (τ).

dx.doi.org/10.1021/jm500457x | J. Med. Chem. XXXX, XXX, XXX–XXX

As previously mentioned in the Introduction, aripiprazole has a high affinity at serotonin receptors, particularly 5-HT_{1A}.[7] Therefore, in light of the structural similarities of aripiprazole with some of our analogues, particularly the biased analogue (**36**), it is worth mentioning that these ligands may also have high affinities at serotonin receptors. As such, the action of these ligands may have an unprecedented complexity of action that should be considered in the characterization of bias not only at the D_2R but also at serotonin receptors as potential dual dopamine−serotonin biased ligands.

We have revealed that the SAR of biased agonism at the D_2R is complex and, depending on the functional scaffold explored, cannot be defined by a single functional group or transformation.[19] The differential bias observed for compounds **18d** and **19** is governed only by the nature of the privileged structure, i.e., **5** or **6**, with the latter conferring bias toward the cAMP assay. For the extended structures, it appears that the 4-methyl-5-chloro-6-methoxy substitution pattern on the thienopyridine scaffold (**34d** and **35**) engenders no bias irrespective of the privileged structure used. However, the 4,6-dimethyl substitution pattern on the thienopyridine motif appears to confer bias regardless of the privileged structure implemented (**36**) (Figure 5). Therefore, for these compounds, this suggests that the bias is driven primarily by the thienopyridine heterocycle and more specifically the substitution pattern upon this heterocycle whereby the influence of the privileged structure is overridden.

CONCLUSION

We explored the determinants of efficacy and affinity for three distinct privileged structures for the D_2R. The privileged structure **7** showed little gain in affinity in both the precursors containing the linkers (**17a−e**) and also the extended structures incorporating an additional thienopyridine heterocycle (**33a−e**). Focusing on the privileged structure **5**, we confirm that the addition of linker groups resulted in a gain in affinity (**18a−e**, Table 1) and in efficacy (Table 3). In particular, we observed a linker length relationship with efficacy with three to five carbon atoms engendering partial agonism (**18b−d**). Inclusion of a heterocyclic structure (**34a−e**) resulted in a different pattern of linker length dependent efficacy, as only extended compounds containing linker lengths of five and six carbon atoms (**34d−e**) exhibited partial agonism. It is therefore likely that compounds that possess only the linker component bind the D_2R in a different orientation to the extended structures incorporating a thienopyridine motif. Extending our studies around the novel partial agonist **34d**, we generated a focused set of compounds that explored the SAR around the two privileged structures **5** and **6**. Of note is that not only can the type of substitution on the phenylpiperazine influence bias, the substitution on the thienopyridine scaffold can have dramatic effects on bias to the point whereby the type of privileged structure used is no longer the principal driver of bias. This observation is consistent with the interaction of the thienopyridine scaffold with a secondary pocket previously identified to interact with other extended D_2R ligands. Our findings suggest that the nature of this interaction confers bias at the D_2R receptor. Our novel D_2R partial agonists **35** and **36** display a similar affinity for the D_2R as aripiprazole but exhibit distinct bias profiles. As such, they may represent useful tools to explore the contribution of biased agonism to antipsychotic efficacy.

EXPERIMENTAL SECTION

Chemistry. All solvents and chemicals were purchased from standard suppliers and were used without any further purification. ^1H NMR and ^{13}C NMR spectra were acquired at 400.13 and 100.62 MHz, respectively, on a Bruker Advance III 400 MHz Ultrashield Plus NMR spectrometer using TOPSPIN 2.1 software. Chemical shifts (δ) for all ^1H spectra are reported in parts per million (ppm) using tetramethylsilane (TMS, 0 ppm) as the reference. The data for all spectra are reported in the following format: chemical shift (δ), (multiplicity, coupling constants J (Hz), integral), where the multiplicity is defined as s = singlet, d = doublet, t = triplet, q = quartet, p = pentet, and m = multiplet. For ^{13}C NMR spectra C = quaternary carbon, CH = methine carbon, CH_2 = methylene carbon, and CH_3 = methyl carbon.

The purity and retention time of final products were determined on an analytical reverse-phase HPLC system fitted with a Luna C8 (2) 100 Å column (50 mm × 4.60 mm, 5 μm) using a binary solvent system: solvent A of 0.1% TFA/H_2O; solvent B of 0.1% TFA/80% MeOH/20% H_2O. Gradient elution was achieved using 100% A for 10 min, 20% A and 80% B over 2 min, and 100% A over 10 min at a flow rate of 1 mL/min monitored at 214 nm using a Waters 996 photodiode array detector.

Thin layer chromatography (TLC) was carried out routinely on silica gel $60F_{254}$ precoated plates (0.25 mm, Merck). Flash column chromatography was carried out using Merck silica gel 60, 230−400 mesh ASTM. Melting points were determined using an electronic MP50 melting point system by Mettler Toledo analytical 2009 and are uncorrected.

Synthesis of Linkers. General Procedure A. The required aminoalkanol **12c−e** (1 equiv) was added to 10−30 mL of dichloromethane. Di-*tert*-butyl dicarbonate (1 equiv) was then added followed by dropwise addition of triethylamine (1.1 equiv) at room temperature. The reaction mixture was stirred for 1 h. After this time, the solvent was removed in vacuo and the resulting oil purified via column chromatography (ethyl acetate).

***tert*-Butyl (4-Hydroxybutyl)carbamate (13c).** **12c** (0.41 mL, 4.49 mmol) and di-*tert*-butyl dicarbonate (979 mg, 4.49 mmol) were added to dichloromethane (10 mL). Triethylamine (0.69 mL, 4.94 mmol) was added dropwise and the mixture stirred for 1 h at room temperature and worked up according to general procedure A. Purification gave the product as a pale yellow oil (809 mg, 95%). ^1H NMR ($CDCl_3$): δ 1.44 (s, 9H), 1.53−1.62 (m, 4H), 2.52 (br s, 1H, OH), 3.14 (m, 2H), 3.65 (m, 2H), 4.78 (br s, 1H, NH). ^{13}C NMR ($CDCl_3$): δ 26.7 (CH_2), 28.5 (CH_3), 29.8 (CH_2), 40.4 (CH_2), 62.3 (CH_2), 79.2 (C), 156.3 (C).

General Procedure B. The required bromoalkanamine **15a,b** (1.1 equiv) was added to 20−30 mL of dichloromethane. Di-*tert*-butyl dicarbonate (1 equiv) was then added followed by dropwise addition of triethylamine (1.1 equiv) at room temperature. The reaction mixture was stirred for 1−1.5 h. After this time, an additional 20 mL of dichloromethane was added and the reaction mixture was washed with 3 × 50 mL portions of saturated potassium hydrogen sulfate solution. The organic layer was then dried over anhydrous sodium sulfate, filtered and the solvent removed to afford the crude product. Further purification of the product was achieved via column chromatography (9:1 petroleum spirits/ethyl acetate).

***tert*-Butyl (2-Bromoethyl)carbamate (16a).** **15a** (1.50 g, 7.32 mmol) and di-*tert*-butyl dicarbonate (1.45 g, 6.66 mmol) were added to dichloromethane (20 mL). Triethylamine (1.02 mL, 7.32 mmol) was added dropwise and the mixture stirred for 1.5 h at room temperature and worked up according to general procedure B to give the product as a colorless oil (413 mg, 28%). ^1H NMR ($CDCl_3$): δ 1.45 (s, 9H), 3.45 (m, 2H), 3.53 (m, 2H), 5.01 (br s, 1H, NH). ^{13}C NMR ($CDCl_3$): δ 28.5 (CH_3), 32.9 (CH_2), 42.5 (CH_2), 80.0 (C), 155.7 (C).

Coupling of Linkers with Privileged Structures 5, 6, and 7. General Procedure C. To a solution of **5** or **7** (1 equiv) in acetonitrile (30 mL) at room temperature under N_2 were added sodium iodide (1 equiv) and *N*,*N*-diisopropylethylamine (2 equiv).

dx.doi.org/10.1021/jm500457x | J. Med. Chem. XXXX, XXX, XXX−XXX

The required Boc protected amines **16a,b** (1.1−1.5 equiv) were dissolved in 1−2 mL of acetonitrile and added slowly to the reaction mixture which was then heated at reflux for 24 h. The reaction was then concentrated in vacuo and the resulting residue partitioned between ethyl acetate (50 mL) and 1 M potassium carbonate (50 mL). The organic layer was removed, and the aqueous layer was further extracted with 2 × 50 mL portions of ethyl acetate. The organic fractions were pooled, washed with water (50 mL), brine (50 mL), dried over anhydrous sodium sulfate, and filtered and the solvent was removed to afford the crude product. Purification is achieved by column chromatography as indicated.

General Procedure D. The Boc protected aminoalkanol **13c−e** (1 equiv) was added to dichloromethane (5 mL). Triethylamine (3 equiv) was added and the reaction mixture cooled to 0 °C via an ice bath. Methanesulfonyl chloride (2 equiv) was then added slowly, and stirring continued for 30 min at 0 °C. After this time the temperature was warmed to room temperature and stirring continued for 1−12 h. The reaction mixture is then diluted with dichloromethane (10 mL), washed with water (3 × 15 mL), dried over anhydrous sodium sulfate, filtered and the solvent removed in vacuo. The mesylates were then reacted immediately with **5**, **6**, or **7** (2−2.5 equiv) in acetonitrile (5 mL) and heated at reflux for 8−24 h. The solvent was then removed in vacuo and the resulting residue redissolved in dichloromethane and washed with saturated sodium bicarbonate (3 × 20 mL). The organic layer was then dried over anhydrous sodium sulfate, filtered, and evaporated to dryness to give the crude product. Further purification was achieved by column chromatography as indicated.

***tert*-Butyl (2-(4-(4-Chlorophenyl)-4-hydroxypiperidin-1-yl)-ethyl)carbamate (17a).** **7** (300 mg, 1.21 mmol), sodium iodide (181 mg, 1.21 mmol), and *N*,*N*-diisopropylethylamine (0.21 mL, 1.21 mmol) were added to acetonitrile (30 mL) at room temperature under N_2. **16a** (350 mg, 1.56 mmol) was then combined with acetonitrile (2 mL) and added slowly to the reaction mixture (full amount added after 1.5 h). After 6 h of reflux, the reaction mixture was worked up as described in general procedure C to give the product as a white foam (348 mg, 81%). Mp: 129.8−131.1 °C. ^{1}H NMR ($CDCl_3$): δ 1.46 (s, 9H), 1.71−1.75 (m, 2H), 2.11 (td, *J* 13.2, 4.3 Hz, 2H), 2.46−2.55 (m, 4H), 2.79 (m, 2H), 3.26 (m, 2H), 5.02 (br s, 1H, NH), 7.31 (m, 2H), 7.44 (m, 2H). ^{13}C NMR ($CDCl_3$): δ 28.6 (CH_3), 38.5 (CH_2), 40.7 (CH_2), 49.4 (CH_2), 57.4 (CH_2), 71.1 (C), 79.4 (C), 126.3 (CH), 128.6 (CH), 133.0 (C), 147.0 (C), 156.1 (C). HPLC purity (λ = 214 nm): 97%, t_R = 7.68 min. HRMS (ESI) TOF (*m*/*z*): $[M + H]^+$ 355.1788 calcd for $C_{18}H_{27}ClN_2O_3$; found $[M + H]^+$ 355.1796.

***tert*-Butyl (6-(4-(4-Chlorophenyl)-4-hydroxypiperidin-1-yl)-hexyl)carbamate (17e).** **7** (292 mg, 1.38 mmol) was added to acetonitrile (5 mL) followed by dropwise addition of **14e** (204 mg, 0.691 mmol). Reflux occurred overnight, and then the reaction mixture was worked up as described in general procedure D to give the product as a white foam (183 mg, 64%). Mp: 64.4−65.7 °C. ^{1}H NMR ($CDCl_3$): δ 1.32−1.35 (m, 4H), 1.44 (s, 9H), 1.48 (m, 2H), 1.54 (m, 2H), 1.73 (m, 2H), 2.15 (m, 2H), 2.39−2.45 (m, 4H), 2.84 (m, 2H), 3.1 (m, 2H), 4.53 (br s, 1H, NH), 7.31 (m, 2H), 7.45 (m, 2H). ^{13}C NMR ($CDCl_3$): δ 26.8 (CH_2), 27.0 (CH_2), 27.4 (CH_2), 28.6 (CH_3), 30.2 (CH_2), 38.5 (CH_2), 40.7 (CH_2), 49.6 (CH_2), 58.9 (CH_2), 71.2 (C), 79.2 (C), 126.3 (CH), 128.6 (CH), 132.9 (C), 147 (C), 156.2 (C). HPLC purity (λ = 214 nm): 95%, t_R = 8.77 min. HRMS (ESI) TOF (*m*/*z*): $[M + H]^+$ 411.2414 calcd for $C_{22}H_{35}ClN_2O_3$; found $[M + H]^+$ 411.2429.

***tert*-Butyl (3-(4-(2-Methoxyphenyl)piperazin-1-yl)propyl)-carbamate (18b).** **5** (200 mg, 0.87 mmol) and *N*,*N*-diisopropylethylamine (0.15 mL, 1.87 mmol) were added to acetonitrile (5 mL) and stirred at room temperature under N_2 for 2 min to generate the free amine. Sodium iodide (131 mg, 0.87 mmol) and additional *N*,*N*-diisopropylethylamine (0.15 mL, 1.87 mmol) were then also added. **16b** (280 mg, 1.18 mmol) was then combined with acetonitrile (2 mL) and added slowly to the reaction mixture. After heating at reflux for 24 h, the reaction mixture was worked up as described in general procedure C and purified via a silica plug (ethanol) to give the product as a colorless oil (286 mg, 93%). ^{1}H NMR ($CDCl_3$): δ 1.44 (s, 9H), 1.70 (p, *J* 6.6 Hz, 2H), 2.49 (t, *J* 6.8 Hz, 2H), 2.65 (m, 4H), 3.10 (m, 4H), 3.22 (m, 2H), 3.86 (s, 3H), 5.49 (br s, 1H, NH), 6.85−7.02 (m, 4H). ^{13}C NMR ($CDCl_3$): δ 26.5 (CH_2), 28.6 (CH_3), 40.2 (CH_2), 50.8 (CH_2), 53.6 (CH_2), 55.5 (CH_3), 57.1 (CH_2), 78.9 (C), 111.3 (CH), 118.3 (CH), 121.1 (CH), 123.0 (CH), 141.4 (C), 152.4 (C), 156.2 (C). HPLC purity (λ = 214 nm): 99%, t_R = 7.74 min. HRMS (ESI) TOF (*m*/*z*): $[M + H]^+$ 350.2444 calcd for $C_{19}H_{31}N_3O_3$; found $[M + H]^+$ 350.2455.

***tert*-Butyl (5-(4-(2-Methoxyphenyl)piperazin-1-yl)pentyl)-carbamate (18d).** **5** (683 mg, 2.99 mmol) was dissolved in acetonitrile (10 mL) and triethylamine (0.21 mL, 1.49 mmol) and stirred for 5 min. **14d** (420 mg, 1.49 mmol) was then added dropwise to the reaction mixture which was refluxed for 24 h. Workup proceeded as described in general procedure D and the crude product was purified by column chromatography (10% chloroform/methanol−100% acetonitrile) to give a yellow/orange oil (334 mg, 59%). ^{1}H NMR ($CDCl_3$): δ 1.36 (m, 2H), 1.44 (s, 9H), 1.47−1.59 (m, 4H), 2.43 (m, 2H), 2.68 (m, 4H), 3.09−3.15 (m, 6H), 3.86 (s, 3H), 4.63 (br s, 1H, NH), 6.84−7.01 (m, 4H). ^{13}C NMR ($CDCl_3$): δ 24.8 (CH_2), 26.4 (CH_2), 28.5 (CH_3), 40.6 (CH_2), 50.5 (CH_2), 53.4 (CH_2), 55.4 (CH_3), 58.6 (CH_2), 79.1 (C), 111.2 (CH), 118.3 (CH), 121.1 (CH), 123.0 (CH), 141.3 (C), 152.3 (C), 156.1 (C). HPLC purity (λ = 214 nm): 98%, t_R = 8.18 min. HRMS (ESI) TOF (*m*/*z*): $[M + H]^+$ 378.2757 calcd for $C_{21}H_{35}N_3O_3$; found $[M + H]^+$ 378.2768.

***tert*-Butyl (5-(4-(2,3-Dichlorophenyl)piperazin-1-yl)pentyl)-carbamate (19).** **6** (1.09 g, 4.07 mmol) was added to acetonitrile (15 mL) followed by **14d** (572 mg, 2.03 mmol) and triethylamine (0.57 mL, 4.07 mmol) and the mixture refluxed for 19 h. Workup proceeded as described in general procedure D and the crude product was purified by column chromatography (chloroform/methanol 99:1) to give a yellow oil (431 mg, 51%). ^{1}H NMR ($CDCl_3$): δ 1.36 (m, 2H), 1.44 (s, 9H), 1.47−1.59 (m, 4H), 2.41 (m, 2H), 2.63 (m, 4H), 3.07 (m, 4H), 3.12 (m, 2H), 4.62 (br s, 1H, NH), 6.96 (m, 1H), 7.12−7.17 (m, 2H). ^{13}C NMR ($CDCl_3$): δ 24.8 (CH_2), 26.6 (CH_2), 28.5 (CH_3), 30.1 (CH_2), 40.6 (CH_2), 51.4 (CH_2), 53.4 (CH_2), 58.6 (CH_2), 79.1 (C), 118.7 (CH), 124.6 (CH), 127.5 (CH), 127.6 (C), 134.1 (C), 151.4 (C), 156.1 (C). HPLC purity (λ = 214 nm): 98%, t_R = 10.43 min. HRMS (ESI) TOF (*m*/*z*): $[M + H]^+$ 416.1872 calcd for $C_{20}H_{31}Cl_2N_3O_2$; found $[M + H]^+$ 416.1870.

Synthesis of Substituted Thienopyridine Scaffolds. 2-Cyanothioacetamide (21). P_4S_{10} (1.00 g, 4.52 mmol) and 2-cyanoacetamide (**20**, 1.00 g, 11.89 mmol) were dissolved in ethyl acetate (12 mL). The mixture was heated at reflux for 1.5−4 h. The reaction mixture was then cooled to room temperature and the orange solid filtered off and washed with ethyl acetate (100 mL). The solid was recrystallized from toluene to give sharp yellow needles (389 mg, ∼30%). ^{1}H NMR (DMSO-d_6): δ 3.98 (s, 2H), 9.48 (s, 1H, NHa), 9.83 (s, 1H, NHb). ^{13}C NMR (DMSO-d_6): δ 33.9 (CH_2), 116.5 (C), 194.5 (C).

4,6-Dimethyl-2-thioxo-1,2-dihydropyridine-3-carbonitrile (22). 2-Cyanothioacetamide (**21**, 1.02 g, 10.2 mmol) and acetylacetone (1.04 mL, 10.2 mmol) were suspended in methanol (10 mL) and warmed until dissolved. Potassium hydroxide (0.75 g) dissolved in methanol (50 mL) was added to the solution, which was stirred for 2 h and then heated at reflux for a further 2 h. The mixture was cooled to room temperature and acidified with 6 M aqueous hydrochloric acid to pH 2−3, and a precipitate resulted. The precipitous mixture was then cooled overnight, filtered, and washed with water. The product was recrystallized from methanol to afford the title compound as yellow needles (1.13 g, 67%). Mp: 266.9−270 °C. ^{1}H NMR (DMSO-d_6): δ 2.34 (s, 3H), 2.35 (s, 3H), 6.69 (s, 1H), 13.83 (br s, 1H). ^{13}C NMR (DMSO-d_6): δ 18.8 (CH_3), 20.8 (CH_3), 113.4 (C), 114.9 (CH), 116.3 (C), 152.6 (C), 156.9 (C), 177.5 (C). HPLC purity (λ = 214 nm): 99%, t_R = 5.56 min.

Ethyl 2-((3-Cyano-4,6-dimethylpyridin-2-yl)thio)acetate (23). Compound **22** (1.00 g, 6.09 mmol) and triethylamine (0.93 mL, 6.70 mmol) were added to *N*,*N*-dimethylformamide (15 mL) and cooled to 0 °C. Ethyl-2-chloroacetate (0.65 mL, 6.09 mmol) was added to 1 mL of *N*,*N*-dimethylformamide and then added dropwise to the reaction mixture. The mixture was then warmed to room temperature for 3.5 h, and a yellow precipitate resulted. The solvent

dx.doi.org/10.1021/jm500457x | J. Med. Chem. XXXX, XXX, XXX−XXX

was then removed and the resulting residue partitioned between dichloromethane (50 mL) and water (50 mL). The organic layer was removed, and the aqueous layer was then washed with further 3 × 50 mL portions of dichloromethane. The organic fractions were combined, dried over anhydrous sodium sulfate, and filtered, and the solvent was removed to leave a yellow solid. Further purification using a silica plug afforded the final compound as a white solid (1.30 g, 86%). ^{1}H NMR (DMSO-d_6): δ 1.17−1.21 (t, J 7.1 Hz, 3H), 2.41 (s, 3H), 2.43 (s, 3H), 4.07 (s, 2H), 4.09- 4.14 (q, J 7.1 Hz, 2H), 7.12 (s, 1H). ^{13}C NMR (DMSO-d_6): δ 14.1 (CH_3), 19.6 (CH_3), 24.2 (CH_3), 32.2 (CH_2), 61.0 (CH_2), 103.6 (C), 114.6 (C), 120.6 (CH), 152.6 (C), 159.7 (C), 161.4 (C), 168.5 (C).

Ethyl 3-Amino-4,6-dimethylthieno[2,3-*b*]pyridine-2-carboxylate (24). **23** (1.29 g, 5.15 mmol) was dissolved in 4−5 mL of *N*,*N*-dimethylformamide followed by 1 M potassium hydroxide (5.15 mL, 5.15 mmol). The reaction mixture was stirred for 15 min at room temperature. Quenching with water (15 mL) caused precipitation of the product that was then filtered to leave a yellow crystalline solid (1.20 g, 93%). Mp: 154.7−155.6 °C. ^{1}H NMR ($CDCl_3$): δ 1.39 (t, J 7.1 Hz, 3H), 2.58 (s, 3H), 2.72 (s, 3H), 4.34 (q, J 7.1 Hz, 2H), 6.14 (br s, 2H, NH_2), 6.84 (s, 1H). ^{13}C NMR ($CDCl_3$): 14.6 (CH_3), 20.3 (CH_3), 24.5 (CH_3), 60.6 (CH_2), 91.2 (C), 121.9 (CH), 122.5 (C), 143.7 (C), 149.1 (C), 159.8 (C), 161.5 (C), 165.9 (C). HPLC purity (λ = 214 nm): 99%, t_R = 8.38 min.

3-Amino-4,6-dimethylthieno[2,3-*b*]pyridine-2-carboxylic Acid (25). To a solution of **24** (1.16 g, 4.62 mmol) in ethanol (15 mL) was added an aqueous solution of sodium hydroxide (2 M, 8 mL), and the mixture was refluxed for 4 h. The solvent was removed in vacuo and the resulting residue dissolved in water (20 mL). Excess aqueous hydrochloric acid (1 M, 10 mL) was added which caused precipitation of the desired compound. Filtration of the precipitate gave the title compound as a yellow solid (856 mg, 83%). Mp: 151.9−152.9 °C. ^{1}H NMR (DMSO-d_6): δ 2.50 (s, 3H), 2.72 (s, 3H), 7.05 (s, 1H). ^{13}C NMR (DMSO-d_6): δ 19.9 (CH_3), 23.4 (CH_3), 95.2 (C), 121.9 (CH), 122.9 (C), 145.8 (C), 149.3 (C), 158.8 (C), 159.0 (C), 166.5 (C).

2-Mercapto-4-methyl-6-oxo-1,6-dihydropyridine-3-carbonitrile (26). A mixture of **21** (8.00 g, 79.89 mmol) and morpholine (6.99 mL, 79.9 mmol) in ethanol (50 mL) was warmed until all components dissolved. Methyl acetoacetate (8.59 mL, 79.9 mmol) was then added and the mixture heated at reflux for 8 h. After cooling to room temperature, the mixture was filtered and the residue washed with cold dichloromethane to give morpholinium 3-cyano-4-methyl-6-oxo-1,6-dihydropyridine-2-thiolate. The desired thiol was isolated by dissolving the thiolate in a minimum amount of water and then acidifying with excess 1 M aqueous hydrochloric acid, which caused precipitation of the molecule. The mixture was refrigerated overnight and then filtered to give the title compound as a pale yellow powder (6.83 g, 51%). Mp: 267−268.9 °C. LRMS (ESI) m/z: 165.1 $[M - H]^+$ (100%).

Ethyl 2-((3-Cyano-4-methyl-6-oxo-1,6-dihydropyridin-2-yl)-thio)acetate (27). Compound **26** (200 mg, 1.2 mmol) and triethylamine (0.18 mL, 1.32 mmol) were added to *N*,*N*-dimethylformamide (8 mL) and cooled to 0 °C. Ethyl 2-chloroacetate (0.13 mL, 1.2 mmol) was added to 1 mL of *N*,*N*-dimethylformamide and then added dropwise to the reaction mixture. The mixture was then warmed to room temperature and stirred for 5 h. The solvent was then removed and the resulting residue dissolved in dichloromethane (50 mL) and partitioned between water (50 mL). The aqueous layer was then washed with further 3 × 50 mL portions of dichloromethane, and the organic layers were combined, dried over anhydrous sodium sulfate, and filtered. The solvent was removed to leave a yellow solid. Further purification by column chromatography afforded the final compound as a white solid (247 mg, 81%). Mp: 102.7−103.5 °C. ^{1}H NMR ($CDCl_3$): δ 1.28 (t, J 7.1 Hz, 3H), 2.38 (d, J 0.9 Hz, 3H), 3.93 (s, 2H), 4.23 (q, J 7.1 Hz, 2H), 6.33−6.35 (m, 1H), 11.03 (br s, 1H, NH). ^{13}C NMR ($CDCl_3$): δ 14.1 (CH_3), 20.9 (CH_3), 34.1 (CH_2), 62.8 (CH_2), 98.2 (C), 113.9 (CH), 114.9 (C), 153.4 (C), 154.3 (C), 163.6 (C), 169.6 (C).

Ethyl 3-Amino-6-methoxy-4-methylthieno[2,3-*b*]pyridine-2-carboxylate (28). Compound **27** (1.52 g, 6.02 mmol) was added to *N*,*N*-dimethylformamide (20 mL) followed by potassium carbonate (1.25 g, 9.04 mmol) and methyl iodide (0.41 mL, 6.63 mmol). The reaction mixture was then stirred at room temperature for 2 h before another 0.5−1 equiv of the methyl iodide was added. After 4 h, 1 M aqueous potassium hydroxide is added and the reaction mixture stirred for 15 min. Water (15 mL) is then added and the resulting white precipitate is filtered and dried overnight over high vacuum (0.91 g, 58%). Mp: 149.5−150.2 °C. ^{1}H NMR ($CDCl_3$): δ 1.38 (t, J 7.1 Hz, 3H), 2.68 (d, J 0.9 Hz, 3H), 3.98 (s, 3H), 4.33 (q, J 7.1 Hz, 2H), 6.11 (br s, 2H, NH_2), 6.43 (m, 1H). ^{13}C NMR ($CDCl_3$): δ 14.7 (CH_3), 20.4 (CH_3), 54.0 (CH_3), 60.4 (CH_2), 95.2 (C), 110.0 (CH), 119.4 (C), 145.9 (C), 149.5 (C), 160.6 (C),164.6 (C), 165.9 (C).

Ethyl 3-(1,3-Dioxoisoindolin-2-yl)-6-methoxy-4-methylthieno[2,3-*b*]pyridine-2-carboxylate (29). To a solution of **28** (65 mg, 0.244 mmol) in acetic acid (5 mL), a total of 4 equiv of phthalic anhydride (150 mg, 1.01 mmol) was added over the 20 h period. The reaction was stopped by cooling the mixture to room temperature and then over an ice bath to initiate precipitation of the final product as a white solid (53 mg, 55%). ^{1}H NMR ($CDCl_3$): δ 1.11 (t, J 7.1 Hz, 3H), 2.37 (s, 3H), 4.02 (s, 3H), 4.20 (q, J 7.1 Hz, 2H), 6.59 (s, 1H), 7.83 (m, 2H), 8.00 (m, 2H). ^{13}C NMR ($CDCl_3$): δ 13.9 (CH_3), 18.5 (CH_3), 54.2 (CH_3), 61.7 (CH_2), 112.2 (CH), 124.2 (CH), 124.7 (C), 125.4 (C), 127.6 (C), 132.4 (C), 134.7 (CH), 145.9 (C), 159.1 (C), 161.1 (C), 164.5 (C), 167.6 (C).

Ethyl 5-Chloro-3-(1,3-dioxoisoindolin-2-yl)-6-methoxy-4-methylthieno[2,3-*b*]pyridine-2-carboxylate (30). Compound **29** (500 mg, 1.26 mmol), *N*-chlorosuccinimide (337 mg, 2.52 mmol), and 3 drops of concentrated HCl were refluxed in acetonitrile (10 mL) for 1.5 h. The solvent was then removed in vacuo and the resulting residue redissolved in chloroform (50 mL) and washed with water (3 × 20 mL) and brine (50 mL). The organic layer was then dried over anhydrous sodium sulfate, filtered, and evaporated to dryness to give the compound as a white solid (506 mg, 93%). ^{1}H NMR ($CDCl_3$): δ 1.12 (t, J 7.1 Hz, 3H), 2.49 (s, 3H), 4.13 (s, 3H), 4.21 (q, J 7.1 Hz, 2H), 7.85 (m, 2H), 8.01 (m, 2H). ^{13}C NMR ($CDCl_3$): δ 13.9 (CH_3), 14.7 (CH_3), 55.4 (CH_3), 61.9 (CH_2), 118.8 (C), 124.3 (CH), 125.1 (C), 127.0 (C), 127.4 (C), 132.4 (C), 134.9 (CH), 143.0 (C), 155.9 (C), 159.5 (C), 160.9 (C), 167.6 (C).

Ethyl 3-Amino-5-chloro-6-methoxy-4-methylthieno[2,3-*b*]-pyridine-2-carboxylate (31). A mixture of **30** (144 mg, 0.33 mmol) and hydrazine monohydrate (65 μL, 1.34 mmol) in ethanol (10 mL) was refluxed for 3 h. Upon cooling to room temperature, the white precipitate was filtered off and washed with cold chloroform (5 mL). The filtrate was then collected and diluted with a further 20 mL of chloroform and washed with water (3 × 20 mL), dried over anhydrous sodium sulfate, and filtered and the solvent removed in vacuo to give the product as a pale yellow solid (85 mg, 84%). ^{1}H NMR ($CDCl_3$): δ 1.38 (t, J 7.1 Hz, 3H), 2.83 (s, 3H), 4.08 (s, 3H), 4.33 (q, J 7.1 Hz, 2H), 6.14 (br s, 2H, NH_2). ^{13}C NMR ($CDCl_3$): δ 14.6 (CH_3), 16.4 (CH_3), 55.2 (CH_3), 60.6 (CH_2), 116.3 (C), 120.1 (C), 142.9 (C), 149.1 (C), 157.3 (C), 159.5 (C), 165.7 (C), 168.4 (C).

3-Amino-5-chloro-6-methoxy-4-methylthieno[2,3-*b*]-pyridine-2-carboxylic Acid (32). Compound **31** (236 mg, 0.783 mmol) was was added to a 50:50 mix of ethanol and 2 M sodium hydroxide. Reflux occurs for 1.5 h before the mixture was cooled to room temperature. An excess of 2 M HCl is added to cause precipitation of the product which is then filtered and washed with a small amount of cold water, giving the product as a beige-yellow solid (179 mg, 84%). ^{1}H NMR (DMSO-d_6): δ 2.77 (s, 3H), 3.96 (s, 3H), 6.41 (br s, 2H, NH_2). LCMS (ESI) m/z: 273.0 $[M + H]^+$ (90%), 275.0 (30%).

General Procedure E for Amide Coupling Reactions Using BOP Reagent. The required carboxylic acids (1 equiv) were added to *N*,*N*-dimethylformamide (10 mL), followed by *N*,*N*-diisopropylethylamine (1.05 equiv) and BOP (1.05 equiv) under N_2 at room temperature and stirred for 5−10 min. The amine (1 equiv) was subsequently added and the reaction mixture stirred at room

dx.doi.org/10.1021/jm500457x | J. Med. Chem. XXXX, XXX, XXX−XXX

temperature for 2−3 h. The solvent was then removed in vacuo and the resulting residue partitioned between dichloromethane (30 mL) and sodium bicarbonate (50 mL). The organic layer was removed, and the aqueous phase was further extracted with 3 × 20 mL portions of dichloromethane. The organic fractions were combined, washed with water (50 mL), brine (50 mL), dried over anhydrous sodium sulfate, filtered, and concentrated to yield the crude product as an oily residue. To remove excess HMPA, crude products are dissolved in ethyl acetate and washed with 3 × 50 mL portions of 2 M brine. Purification of the product was performed by column chromatography and/or recrystalisation as indicated.

3-Amino-*N*-(2-(4-(4-chlorophenyl)-4-hydroxypiperidin-1-yl)-ethyl)-4,6-dimethylthieno[2,3-*b*]pyridine-2-carboxamide (33a). Carboxylic acid **25** (50 mg, 0.225 mmol), *N*,*N*-diisopropylethylamine (0.041 mL, 0.24 mmol), and BOP (104 mg 0.24 mmol) were added to *N*,*N*-dimethylformamide (2 mL). **17a** (92 mg, 0.28 mmol) was dissolved in 2 mL of *N*,*N*-dimethylformamide and *N*,*N*-diisopropylethylamine (0.078 mL, 0.450 mmol) and then added to the reaction mixture. After the mixture was stirred for 16 h at room temperature, the crude product was worked up as per general procedure E to give an amber solid (32 mg, 31%). Mp: 159−163 °C. ^{1}H NMR (DMSO-d_6): δ 1.58 (d, J 12.1 Hz, 2H), 1.91 (td, J 12.9, 4.1 Hz, 2H), 2.44−2.53 (m, 7H), 2.71−2.72 (m, 5H), 3.36 (m, 2H), 4.9 (s, 1H, OH), 6.78 (s, 2H, NH_2), 7.02 (s, 1H), 7.36 (m, 2H), 7.50 (m, 2H), 7.55 (t, J 5.5 Hz, 1H, NH). ^{13}C NMR (DMSO-d_6): δ 19.7 (CH_3), 23.8 (CH_3), 36.7 (CH_2), 37.9 (CH_2), 49.1 (CH_2), 57.2 (CH_2), 69.4 (C), 97.6 (C), 121.8 (CH), 123.2 (C), 126.8 (CH), 127.7 (CH), 130.8 (C), 144.5 (C), 147.5 (C), 149.1 (C), 158.4 (C), 158.5 (C), 165.2 (C). HPLC purity (λ = 214 nm): 98%, t_R = 8.06 min. HRMS (ESI) TOF (m/z): [M + H]$^+$ 459.1621 calcd for $C_{23}H_{27}ClN_4O_2S$; found [M + H]$^+$ 459.1634.

3-Amino-*N*-(6-(4-(4-chlorophenyl)-4-hydroxypiperidin-1-yl)-hexyl)-4,6-dimethylthieno[2,3-*b*]pyridine-2-carboxamide (33e). Carboxylic acid **25** (61 mg, 0.274 mmol), *N*,*N*-diisopropylethylamine (0.146 mL, 0.837 mmol), and BOP (128 mg, 0.288 mmol) were added to *N*,*N*-dimethylformamide (2 mL). **17e** (116 mg, 0.302 mmol) was dissolved in 2 mL of *N*,*N*-dimethylformamide and *N*,*N*-diisopropylethylamine (0.096 mL, 0.550 mmol) and then added to the reaction mixture. After the mixture was stirred for 5 h at room temperature, the crude product was worked up as per general procedure E to give the product as a pale yellow solid (49 mg, 35%). Mp: 137.2−140.3 °C. ^{1}H NMR ($CDCl_3$): δ 1.39−1.42 (m, 4H), 1.57−1.65 (m, 4H), 1.72−7.75 (m, 3H), 2.19 (m, 2H), 2.43−2.5 (m, 4H), 2.58 (s, 3H), 2.74 (s, 1H), 2.87 (m, 2H), 3.42 (dd, J 13.1, 7 Hz, 2H), 5.55 (t, J 5.3 Hz, 1H, NH), 6.3 (s, 2H, NH_2), 6.87 (s, 1H), 7.29 (m, 2H), 7.44 (m, 2H). ^{13}C NMR ($CDCl_3$): δ 20.2 (CH_3), 24.3 (CH_3), 26.8 (CH_2), 27.0 (CH_2), 27.4 (CH_2), 29.9 (CH_2), 38.4 (CH_2), 39.8 (CH_2), 49.5 (CH_2), 58.7 (CH_2), 71.1 (C), 98.7 (C), 122.3 (CH), 123.8 (C), 126.3 (CH), 128.5 (CH), 132.9 (C), 143.8 (C), 147.0 (C), 147.3 (C), 159.1 (C), 159.2 (C), 166 (C). HPLC purity (λ = 214 nm): 98%, t_R = 8.39 min. HRMS (ESI) TOF (m/z): [M + H]$^+$ 515.2247 calcd for $C_{27}H_{35}ClN_4O_2S$; found [M + H]$^+$ 515.2254.

3-Amino-5-chloro-6-methoxy-*N*-(4-(4-(2-methoxyphenyl)-piperazin-1-yl)butyl)-4-methylthieno[2,3-*b*]pyridine-2-carboxamide (34c). Carboxylic acid **32** (100 mg, 0.367 mmol), *N*,*N*-diisopropylethylamine (0.067 mL, 0.385 mmol), and BOP (176 mg, 0.398 mmol) were added to *N*,*N*-dimethylformamide (10 mL). **18c** (121 mg, 0.403 mmol) was dissolved in 2 mL of *N*,*N*-dimethylformamide, and *N*,*N*-diisopropylethylamine (0.077 mL, 0.403 mmol) was then added to convert to the free base, which was added dropwise to the reaction mixture. The reaction mixture was then worked up as described in general procedure E to give the product as a tan crystalline solid (55 mg, 29%). Mp: 99.1−101.6 °C (methanol/water). ^{1}H NMR ($CDCl_3$): δ 1.62−1.69 (m, 4H), 2.46 (m, 2H), 2.67 (m, 4H), 2.80 (s, 3H), 3.11 (m, 4H), 3.44 (q, J 6.5 Hz, 2H), 3.86 (s, 3H), 4.06 (s, 3H), 5.66 (t, J 5.6 Hz, 1H, NH), 6.28 (s, 2H, NH_2), 6.84−7.01 (m, 4H). ^{13}C NMR ($CDCl_3$): δ 16.4 (CH_3), 24.4 (CH_2), 27.0 (CH_2), 39.7 (CH_2), 50.8 (CH_2), 53.7 (CH_2), 55.2 (CH_3), 55.5 (CH_3), 58.3 (CH_2), 98.4 (C), 111.3 (CH), 116.6 (C), 118.4 (CH), 121.1 (CH), 121.3 (C), 123.1 (CH), 141.5 (C), 143.1 (C), 147.4 (C), 152.4 (C), 154.5 (C), 159.3 (C), 165.8 (C). HPLC purity (λ = 214 nm): 97%, t_R = 9.30 min. HRMS (ESI) TOF (m/z): [M + H]$^+$ 518.1993 calcd for $C_{25}H_{32}ClN_5O_3S$; found [M + H]$^+$ 518.2005.

3-Amino-5-chloro-6-methoxy-*N*-(5-(4-(2-methoxyphenyl)-piperazin-1-yl)pentyl)-4-methylthieno[2,3-*b*]pyridine-2-carboxamide (34d). Carboxylic acid **32** (100 mg, 0.367 mmol), *N*,*N*-diisopropylethylamine (0.067 mL, 0.385 mmol), and BOP (170 mg, 0.385 mmol) were added to *N*,*N*-dimethylformamide (10 mL). **18d** (127 mg, 0.403 mmol) was dissolved in 2 mL of *N*,*N*-dimethylformamide, and *N*,*N*-diisopropylethylamine (0.11 mL, 0.403 mmol) was then added to convert to the free base, which was added dropwise to the reaction mixture. The reaction mixture was then worked up as described in general procedure E to give the product as pale red microneedles (97 mg, 50%). Mp: 96−97.7 °C (methanol/water). ^{1}H NMR ($CDCl_3$): δ 1.43 (m, 2H), 1.56−1.69 (m, 4H), 2.43 (m, 2H), 2.66 (m, 4H), 2.83 (s, 3H), 3.10 (m, 4H), 3.42 (m, 2H), 3.86 (s, 3H), 4.07 (s, 3H), 5.44 (t, J 5.6 Hz, 1H, NH), 6.30 (br s, 2H, NH_2), 6.84−7.02 (m, 4H). ^{13}C NMR ($CDCl_3$): δ 16.4 (CH_3), 25.1 (CH_2), 26.7 (CH_2), 29.9 (CH_2), 39.7 (CH_2), 50.8 (CH_2), 53.6 (CH_2), 55.2 (CH_3), 55.5 (CH_3), 58.7 (CH_2), 98.3 (C), 111.3 (CH), 116.6 (C), 118.3 (CH), 121.1 (CH), 121.3 (C), 123.0 (CH), 141.5 (C), 143.1 (C), 147.4 (C), 152.4 (C), 154.4 (C), 159.3 (C), 165.8 (C). HPLC purity (λ = 214 nm): 99%, t_R = 9.84 min. HRMS (ESI) TOF (m/z): [M + H]$^+$ 532.2149 calcd for $C_{26}H_{34}ClN_5O_3S$; found [M + H]$^+$ 532.2166.

3-Amino-5-chloro-*N*-(5-(4-(2,3-dichlorophenyl)piperazin-1-yl)pentyl)-6-methoxy-4-methylthieno[2,3-*b*]pyridine-2-carboxamide (35). Carboxylic acid 32 (80 mg, 0.293 mmol), *N*,*N*-diisopropylethylamine (0.05 mL, 0.308 mmol), and BOP (136 mg, 0.308 mmol) were added together. Compound **19**, which was Boc deprotected and isolated as the HCl salt (114 mg, 0.298 mmol), was dissolved in 2 mL of *N*,*N*-dimethylformamide, and *N*,*N*-diisopropylethylamine (0.05 mL) was then added to convert to the free base, which was added dropwise to the reaction mixture. The reaction mixture was then worked up as described in general procedure E to give the product as a beige solid (106 mg, 63%). Mp: 114.5−116.5 °C. ^{1}H NMR ($CDCl_3$): δ 1.41 (m, 2H), 1.57−1.67 (m, 4H), 2.44 (m, 2H), 2.64 (m, 4H), 2.81 (s, 3H), 3.07 (m, 4H), 3.42 (m, 2H), 4.06 (s, 3H), 5.48 (t, J 5.7 Hz, 1H, NH), 6.30 (br s, 2H, NH_2), 6.94 (dd, J 7.2, 2.4, 1H), 7.10−7.16 (m, 2H). ^{13}C NMR ($CDCl_3$): δ 16.3 (CH_3), 24.9 (CH_2), 26.6 (CH_2), 29.9 (CH_2), 39.7 (CH_2), 51.3 (CH_2), 53.4 (CH_2), 55.1 (CH_3), 58.5 (CH_2), 98.2 (C), 116.5 (C), 118.7 (CH), 121.2 (C), 124.6 (CH), 127.5 (CH), 127.5 (C), 134.1 (C), 143.0 (C), 147.3 (C), 151.4 (C), 154.3 (C), 159.2 (C), 165.7 (C). HPLC purity (λ = 214 nm): 99%, t_R = 11.66 min. HRMS (ESI) TOF (m/z): [M + H]$^+$ 570.1264 calcd for $C_{25}H_{30}Cl_3N_5O_2S$; found [M + H]$^+$ 570.1265.

3-Amino-*N*-(5-(4-(2,3-dichlorophenyl)piperazin-1-yl)pentyl)-4,6-dimethylthieno[2,3-*b*]pyridine-2-carboxamide (36). Carboxylic acid **25** (73 mg, 0.32 mmol), *N*,*N*-diisopropylethylamine (0.059 mL, 0.34 mmol), and BOP (150 mg, 0.34 mmol) were added to *N*,*N*-dimethylformamide (2 mL). Compound **19**, which was Boc deprotected and isolated as the HCl salt (126 mg, 0.36 mmol), was dissolved in 2 mL of *N*,*N*-dimethylformamide and *N*,*N*-diisopropylethylamine (0.062 mL, 0.36 mmol) and then added to the reaction mixture. The reaction mixture was then worked up as described in general procedure E to give the product as a fluffy beige solid (119 mg, 70%). Mp: 142.9−143.8 °C. ^{1}H NMR ($CDCl_3$): δ 1.42 (m, 2H), 1.57−1.67 (m, 4H), 2.44 (m, 2H), 2.58 (s, 3H), 2.63 (m, 4H), 2.73 (s, 3H), 3.07 (m, 4H), 3.42 (m, 2H), 5.59 (t, J 5.6, 1H, NH), 6.31 (br s, 2H, NH_2), 6.86 (s, 1H), 6.94 (dd, J 7.0, 2.6 Hz, 1H), 7.10−7.15 (m, 2H). ^{13}C NMR ($CDCl_3$): δ 20.3 (CH_3), 24.4 (CH_3), 24.9 (CH_2), 26.6 (CH_2), 29.9 (CH_2), 39.7 (CH_2), 51.4 (CH_2), 53.4 (CH_2), 58.5 (CH_2), 98.6 (C), 118.7 (CH), 122.3 (CH), 123.7 (C), 124.6 (CH), 127.5 (CH), 127.6 (C), 134.1 (C), 143.7 (C), 147.3 (C),151.4 (C), 159.0 (C), 159.1 (C), 165.9 (C). HPLC purity (λ = 214 nm): 99%, t_R = 10.13 min. HRMS (ESI) TOF (m/z): [M + H]$^+$ 520.1705 calcd for $C_{25}H_{31}Cl_2N_5OS$; found [M + H]$^+$ 520.1703.

3-Amino-*N*-(5-(4-(2-methoxyphenyl)piperazin-1-yl)pentyl)-4,6-dimethylthieno[2,3-*b*]pyridine-2-carboxamide (37). Carboxylic acid **25** (80 mg, 0.36 mmol), *N*,*N*-diisopropylethylamine

dx.doi.org/10.1021/jm500457x | J. Med. Chem. XXXX, XXX, XXX−XXX

(0.066 mL, 0.38 mmol), and BOP (167 mg, 0.38 mmol) were added to *N*,*N*-dimethylformamide (2 mL). **18d** (124 mg, 0.40 mmol) was dissolved in 2 mL of *N*,*N*-dimethylformamide and *N*,*N*-diisopropylethylamine (0.069 mL, 0.40 mmol) and then added to the reaction mixture. The reaction mixture was then worked up as described in general procedure E to give the product as a yellow-orange solid (66 mg, 38%). Mp: 127.6−128.2 °C. ^{1}H NMR ($CDCl_3$): δ 1.42 (m, 2H), 1.57−1.67 (m, 4H), 2.53 (m, 2H), 2.58 (s, 3H), 2.72 (s, 3H), 2.77 (m, 4H), 3.14 (m, 4H), 3.40 (m, 2H), 3.85 (s, 3H), 5.64 (t, *J* 5.7, 1H, NH), 6.30 (br s, 2H, NH_2), 6.84−7.02 (m, 5H). ^{13}C NMR ($CDCl_3$): δ 20.2 (CH_3), 24.4 (CH_3), 24.8 (CH_2), 26.1 (CH_2), 29.8 (CH_2), 39.6 (CH_2), 50.2 (CH_2), 53.5 (CH_2), 55.5 (CH_3), 58.5 (CH_2), 98.7 (C), 111.3 (CH), 118.4 (CH), 121.1 (CH), 122.3 (CH), 123.2 (CH), 123.7 (C), 141.0 (C), 143.7 (C), 147.3 (C), 152.3 (C), 159.0 (C), 159.1 (C), 166.0 (C). HPLC purity (λ = 214 nm): 97%, t_R = 8.89 min. HRMS (ESI) TOF (m/z): $[M + H]^+$ 482.2590 calcd for $C_{26}H_{35}N_5O_2S$; found $[M + H]^+$ 482.2590.

Pharmacology. Cell Lines and Transfection. FlpIn CHO cells (Invitrogen) were grown in Dulbecco's modified Eagle medium (DMEM) supplemented with 10% fetal bovine serum and maintained at 37 °C in a humidified incubator containing 5% CO_2. The FlpIn CHO cells were transfected with the pOG44 vector encoding Flp recombinase and the pDEST vector encoding the wild-type long isoform of the human D_2 receptor ($D_{2L}R$) at a ratio of 9:1 using polyethylenimine as the transfection reagent. At 24 h after transfection, the cells were subcultured, and the medium was supplemented with 700 μg/mL HygroGold as a selection agent. Cells were grown and maintained in DMEM containing 20 mM HEPES, 5% fetal bovine serum, and 200 μg/mL hygromycin B. Cells were maintained at 37 °C in a humidified incubator containing 5% CO_2 and 95% O_2.

Preparation of FlpIN CHO Cell Membranes. When cells were approximately 90% confluent, they were harvested and centrifuged (300*g*, 3 min). The resulting pellet was resuspended in assay buffer (20 mM HEPES, 100 mM NaCl, 6 mM $MgCl_2$, 1 mM EGTA, and 1 mM EDTA, pH 7.4), and the centrifugation procedure was repeated. The intact cell pellet was then resuspended in assay buffer and homogenized using a Polytron homogenizer for three 10 s intervals on the maximum setting, with 30 s periods on ice between each burst. The homogenate volume was brought up to 30 mL. The sample was centrifuged (1000*g*, 10 min, 25 °C). The pellet was discarded, and the supernatant was recentrifuged at 30 000*g* for 1 h at 4 °C. The resulting pellet was resuspended in 5 mL of assay buffer, and the protein content was determined using the method of Bradford. The homogenate was then separated into 0.5 mL aliquots and stored frozen at −80 °C until it was required for binding assays.

[^{3}H]Spiperone Binding Assay. Cell membranes (D_{2L}-FlpIn CHO, 3 μg) were incubated with varying concentrations of test compound in binding buffer (20 mM HEPES, 100 mM NaCl, 6 mM $MgCl_2$, 1 mM EGTA, and 1 mM EDTA, pH 7.4) containing 0.05 nM of [^{3}H]spiperone and 100 μM GppNHp to a final volume of 1 mL and were incubated at 37 °C for 3 h. Binding was terminated by fast-flow filtration over GF/B membranes using a Brandel harvester followed by three washes with ice-cold 0.9% NaCl. Bound radioactivity was measured in a Tri-Carb 2900TR liquid scintillation counter (PerkinElmer).

ERK1/2 Phosphorylation Assay. FlpIn CHO cells stably expressing the $D_{2L}R$ were seeded into 96-well plates at a density of 50 000 cells/well. After 5 h, cells were washed with phosphate buffered saline (PBS) and incubated in serum-free DMEM overnight before assaying. Initially, time-course experiments were conducted at least twice for each ligand to determine the time required to maximally promote ERK1/2 phosphorylation via the dopamine $D_{2L}R$. Dose−response experiments were performed in the absence and presence of increasing concentrations of each ligand at 37 °C. Stimulation of the cells was terminated by removing the media followed by the addition of 100 μL of SureFire lysis buffer (PerkinElmer) to each well. The plate was shaken for 5 min at room temperature before transferring 5 μL of the lysates to a white 384-well Proxiplate (PerkinElmer). Then 8 μL of a 240:1440:7:7 mixture of Surefire activation buffer/Surefire reaction buffer/Alphascreen acceptor beads/Alphascreen donor beads was added to the samples and incubated in the dark at 37 °C for 1.5 h. Plates were read using a Fusion plate reader.

cAMP Accumulation Assays. The cells were grown and incubated overnight and then preincubated for 45 min in 80 μL of stimulation buffer (Hank's buffered salt solution: 0.14 M NaCl, 5.4 mM KCl, 0.8 μM $MgSO_4$, 1.3 mM $CaCl_2$, 0.2 mM Na_2HPO_4, 0.44 mM KH_2PO_4, 5.6 mM D-glucose, 1 mg/mL BSA, 0.5 mM 3-isobutyl-1-methylxanthine, and 5 mM HEPES, pH 7.4). The agonists (10 μL) and 300 nM forskolin (10 μL) were added simultaneously to the cells and incubated for 30 min at 37 °C. Stimulation was terminated via the removal of the stimulation buffer and addition of 50 μL of ice cold 100% ethanol. The plates were then incubated at 37 °C to allow evaporation of the ethanol. Then 50 μL of detection buffer (1 mg/mL BSA, 0.3% Tween-20, and 5 mM HEPES, pH 7.4) was added and 5 μL of each well transferred to a 384-well Optiplate (PerkinElmer, Waltham, MA, U.S.). Anti-cAMP acceptor beads (0.2 units/μL) diluted in stimulation buffer was added under green light for 30 min before the addition of 15 μL of the donor beads/biotinylated cAMP (0.07 units/μL) diluted in detection buffer. The plates were incubated for 1 h at room temperature and read using a Fusion-α plate reader using AlphaScreen presettings.

Inhibition Assays for Analogues 5, 18a, and 18e. The required analogues were added to the cells at the appropriate dilutions and incubated at 37 °C for 30 min before the addition of 10 nM dopamine. After an additional 5 min stimulation time, termination of the ERK1/2 phosphorylation was as stated above.

Concentration−Response Assays for Analogues 18b−d, 19, 34d, 35, and 36. The required analogues were added to the cells at the appropriate dilutions and incubated at 37 °C for 5−10 min as predetermined for each compound in the time-course assays. Termination of the ERK1/2 phosphorylation was as stated above.

Interaction Studies with Dopamine for Compounds 34a−e. The required analogues and dopamine were added to the cells simulataneously at the appropriate dilutions and incubated at 37 °C for 5 min. Termination of the ERK1/2 phosphorylation was as stated above.

Data Analysis. Computerized nonlinear regression was performed using Prism 6.0 (GraphPad Software, San Diego, CA).

Agonist concentration−response curves were fitted via nonlinear regression to the three-parameter logistic function (eq 1):

$$E = \text{basal} + \frac{E_{max} - \text{basal}}{1 + 10^{(-pEC_{50} - \log[A])}} \quad (1)$$

where E is response, E_{max} and basal are the top and bottom asymptotes of the curve, respectively, log[A] is the logarithm of the agonist concentration, and pEC_{50} is the negative logarithm of the agonist concentration that gives a response halfway between E_{max} and basal.

To compare agonist profiles and quantify stimulus bias, agonist concentration−response curves were fitted to the following form of the operational model of agonism (eq 2):

$$Y = \text{basal} + \frac{(E_m - \text{basal})\left(\frac{\tau}{K_A}\right)^n [A]^n}{[A]^n \left(\frac{\tau}{K_A}\right)^n + \left(1 + \frac{[A]}{K_A}\right)^n} \quad (2)$$

where E_m is the maximal possible response of the system; basal is the basal level of response; K_A denotes the equilibrium dissociation constant of the agonist (A); τ is an index of the signaling efficacy of the agonist and is defined as R_T/K_E, where R_T is the total number of receptors and K_E is the coupling efficiency of each agonist-occupied receptor; and n is the slope of the transducer function that links occupancy to response. The analysis assumes that the maximal system responsiveness (E_m) and the transduction machinery utilized for a given cellular pathway are the same for all agonists such that the E_m and transducer slope (n) are shared between agonists. The ratio τ/K_A (determined as a logarithm, i.e., $\log(\tau/K_A)$) is referred to herein as the "transduction coefficient", as this composite parameter is sufficient to describe agonism and bias for a given pathway; i.e., stimulus-biased agonism can result from either a selective affinity ($K_{A\text{-}1}$) of an agonist

dx.doi.org/10.1021/jm500457x | J. Med. Chem. XXXX, XXX, XXX−XXX

for a given receptor state(s) and/or a differential coupling efficacy (τ) toward certain pathways. To cancel the impact of cell-dependent effects on the observed agonism at each pathway, the $\log(\tau/K_A)$ values were then normalized to that determined for the endogenous agonist dopamine at each pathway to yield a "normalized transduction coefficient", $\Delta\log(\tau/K_A)$, i.e., $\Delta\log(\tau/K_A) = \log(\tau/K_A)_{test} - \log(\tau/K_A)_{dopamine}$.

To determine the actual bias of each agonist for different signaling pathways, the $\Delta\log(\tau/K_A)$ values were evaluated statistically between the pathways. The ligand bias of an agonist for one pathway, j1, over another, j2 is given as (eq 3)

$$\Delta\Delta\log\left(\frac{\tau}{K_A}\right)_{j1-j2} = \Delta\log\left(\frac{\tau}{K_A}\right)_{j1} - \Delta\log\left(\frac{\tau}{K_A}\right)_{j2} \quad (3)$$

A lack of stimulus bias compared to a reference agonist (in this case dopamine) will result in values of $\Delta\Delta\log(\tau/K_A)$ not significantly different from 0 between pathways. To account for the propagation of error associated with the determination of composite parameters, eq 5 was used:

$$\text{SEM} = \frac{\sigma}{\sqrt{n}} \quad (4)$$

where σ is the standard deviation and n is the number of experiments,

$$\text{pooled SEM} = \sqrt{(\text{SEM1})^2 + (\text{SEM2})^2} \quad (5)$$

All affinity, potency, and transduction ratio parameters were estimated as logarithms. All results are expressed as the mean ± SEM. Statistical analyses were performed where appropriate using one-way ANOVA with the Tukey's post hoc test. Statistical significance was taken as $p < 0.05$. For a more detailed explanation and analysis of using bias calculations see van der Westhuizen et al.[33]

■ ASSOCIATED CONTENT

Supporting Information

Values of potency (pEC_{50}) and maximal stimulation (E_{max}) for dopamine, aripiprazole, **18d**, **19**, **34d**, and **35**−**37** for cAMP and pERK1/2 signaling assays; full experimental and characterization of compounds **13d**−**e**, **16b**, **17b**−**d**, **18a**,**c**,**e**, **33b**−**d**, **34a**,**b**,**e**. This material is available free of charge via the Internet at http://pubs.acs.org.

■ AUTHOR INFORMATION

Corresponding Authors

*J.R.L.: phone, +613 9903 9095; fax, +613 9903 9581; e-mail, rob.lane@monash.edu.

*B.C.: phone, +61 3 9903 9556; fax, +61 3 9903 9581; e-mail, ben.capuano@monash.edu.

Notes

The authors declare no competing financial interest.

■ ACKNOWLEDGMENTS

This research was supported by Project Grants 1049564 and 1011920 of the National Health and Medical Research Council (NHMRC). A.C. is a Principle Research Fellow (NHMRC). J.R.L. is a R. D. Wright Biomedical Career Development Fellow (Grant 1052304, NHMRC) and a Larkin's Fellow (Monash University, Australia). M.S. acknowledges an Australian postgraduate award. C.K.H. acknowledges a Monash graduate scholarship. Special thanks are given to Dr. Jason Dang for running HRMS on final compounds.

■ ABBREVIATIONS USED

GPCR, G-protein-coupled receptor; CNS, central nervous system; TLC, thin layer chromatography; ERK, extracellular signal-regulated kinase; cAMP, cyclic adenosine monophosphate; FSK, forskolin; Boc, *tert*-butyloxycarbonyl; NMR, nuclear magnetic resonance; BOP, (benzotriazol-1-yloxy)tris-(dimethylamino)phosphonium hexafluorophosphate

■ REFERENCES

(1) Missale, C.; Nash, S. R.; Robinson, S. W.; Jaber, M.; Caron, M. G. Dopamine receptors: from structure to function. *Physiol. Rev.* **1998**, *78*, 189−225.

(2) Seeman, P. Targeting the dopamine D2 receptor in schizophrenia. *Expert Opin. Ther. Targets* **2006**, *10*, 515−531.

(3) Shin, J. K.; Malone, D. T.; Crosby, I. T.; Capuano, B. Schizophrenia: a systematic review of the disease state, current therapeutics and their molecular mechanisms of action. *Curr. Med. Chem.* **2011**, *18*, 1380−1404.

(4) Tandon, R. Pharmacologic treatment of schizophrenia: current status and future trends. *Curr. Psychosis Ther. Rep.* **2006**, *4*, 40−49.

(5) Rosen, W. G.; Mohs, R. C.; Johns, C. A.; Small, N. S.; Kendler, K. S.; Horvath, T. B.; Davis, K. L. Positive and negative symptoms in schizophrenia. *Psychiatry Res.* **1984**, *13*, 277−284.

(6) Inoue, T.; Domae, M.; Yamada, K.; Furukawa, T. Effects of the novel antipsychotic agent 7-(4-[4-(2,3-dichlorophenyl)-1-piperazinyl]-butyloxy)-3,4-dihydro-2(1*H*)-quinolinone (OPC-14597) on prolactin release from the rat anterior pituitary gland. *J. Pharmacol. Exp. Ther.* **1996**, *277*, 137−143.

(7) Jordan, S.; Koprivica, V.; Chen, R.; Tottori, K.; Kikuchi, T.; Altar, C. A. The antipsychotic aripiprazole is a potent, partial agonist at the human 5-HT1A receptor. *Eur. J. Pharmacol.* **2002**, *441*, 137−140.

(8) Shapiro, D. A.; Renock, S.; Arrington, E.; Chiodo, L. A.; Liu, L.-X.; Sibley, D. R.; Roth, B. L.; Mailman, R. Aripiprazole, a novel atypical antipsychotic drug with a unique and robust pharmacology. *Neuropsychopharmacology* **2003**, *28*, 1400−1411.

(9) Tamminga, C. A. Partial dopamine agonists in the treatment of psychosis. *J. Neural Transm.* **2002**, *109*, 411−420.

(10) Kenakin, T. Functional selectivity and biased receptor signaling. *J. Pharmacol. Exp. Ther.* **2011**, *336*, 296−302.

(11) Kenakin, T.; Christopoulos, A. Signalling bias in new drug discovery: detection, quantification and therapeutic impact. *Nat. Rev. Drug Discovery* **2013**, *12*, 205−216.

(12) Stallaert, W.; Christopoulos, A.; Bouvier, M. Ligand functional selectivity and quantitative pharmacology at G protein-coupled receptors. *Expert Opin. Drug Discovery* **2011**, *6*, 811−825.

(13) Urban, J. D.; Vargas, G. A.; von Zastrow, M.; Mailman, R. B. Aripiprazole has functionally selective actions at dopamine D2 receptor-mediated signaling pathways. *Neuropsychopharmacology* **2006**, *32*, 67−77.

(14) Allen, J. A.; Yost, J. M.; Setola, V.; Chen, X.; Sassano, M. F.; Chen, M.; Peterson, S.; Yadav, P. N.; Huang, X.-p.; Feng, B.; Jensen, N. H.; Che, X.; Bai, X.; Frye, S. V.; Wetsel, W. C.; Caron, M. G.; Javitch, J. A.; Roth, B. L.; Jin, J. Discovery of β-arrestin-biased dopamine D2 ligands for probing signal transduction pathways essential for antipsychotic efficacy. *Proc. Natl. Acad. Sci. U.S.A.* **2011**, *108*, 18488−18493.

(15) Chen, X.; Sassano, M. F.; Zheng, L.; Setola, V.; Chen, M.; Bai, X.; Frye, S. V.; Wetsel, W. C.; Roth, B. L.; Jin, J. Structure−functional selectivity relationship studies of β-arrestin-biased dopamine D2 receptor agonists. *J. Med. Chem.* **2012**, *55*, 7141−7153.

(16) Gay, E. A.; Urban, J. D.; Nichols, D. E.; Oxford, G. S.; Mailman, R. B. Functional selectivity of D2 receptor ligands in a Chinese hamster ovary hD2L cell line: evidence for induction of ligand-specific receptor states. *Mol. Pharmacol.* **2004**, *66*, 97−105.

(17) Mottola, D. M.; Kilts, J. D.; Lewis, M. M.; Connery, H. S.; Walker, Q. D.; Jones, S. R.; Booth, R. G.; Hyslop, D. K.; Piercey, M.; Wightman, R. M.; Lawler, C. P.; Nichols, D. E.; Mailman, R. B. Functional selectivity of dopamine receptor agonists. I. Selective activation of postsynaptic dopamine D2 receptors linked to adenylate cyclase. *J. Pharmacol. Exp. Ther.* **2002**, *301*, 1166−1178.

(18) Tschammer, N.; Bollinger, S.; Kenakin, T.; Gmeiner, P. Histidine 6.55 is a major determinant of ligand-biased signaling in dopamine D2L receptor. *Mol. Pharmacol.* **2011**, *79*, 575−585.
(19) Shonberg, J.; Herenbrink, C. K.; López, L.; Christopoulos, A.; Scammells, P. J.; Capuano, B.; Lane, J. R. A structure−activity analysis of biased agonism at the dopamine D2 receptor. *J. Med. Chem.* **2013**, *56*, 9199−9221.
(20) DeSimone, R. W.; Currie, K. S.; Mitchell, S. A.; Darrow, J. W.; Pippin, D. A. Privileged structures: applications in drug discovery. *Comb. Chem. High Throughput Screening* **2004**, *7*, 473−493.
(21) Costantino, L.; Barlocco, D. Privileged structures as leads in medicinal chemistry. *Curr. Med. Chem.* **2010**, *5*, 381−422.
(22) Duarte, C. D.; Barreiro, E. J.; Fraga, C. A. M. Privileged structures: a useful concept for the rational design of new lead drug candidates. *Mini-Rev. Med. Chem.* **2007**, *7*, 1108−1119.
(23) Bondensgaard, K.; Ankersen, M.; Thøgersen, H.; Hansen, B. S.; Wulff, B. S.; Bywater, R. P. Recognition of privileged structures by G-protein coupled receptors. *J. Med. Chem.* **2004**, *47*, 888−899.
(24) Kulagowski, J. J.; Broughton, H. B.; Curtis, N. R.; Mawer, I. M.; Ridgill, M. P.; Baker, R.; Emms, F.; Freedman, S. B.; Marwood, R.; Patel, S.; Patel, S.; Ragan, C. I.; Leeson, P. D. 3-[[4-(4-Chlorophenyl)-piperazin-1-yl]methyl]-1*H*-pyrrolo[2,3-*b*]pyridine: an antagonist with high affinity and selectivity for the human dopamine D4 receptor. *J. Med. Chem.* **1996**, *39*, 1941−1942.
(25) Löber, S.; Hübner, H.; Tschammer, N.; Gmeiner, P. Recent advances in the search for D3- and D4-selective drugs: probes, models and candidates. *Trends Pharmacol. Sci.* **2011**, *32*, 148−157.
(26) Newman, A. H.; Beuming, T.; Banala, A. K.; Donthamsetti, P.; Pongetti, K.; LaBounty, A.; Levy, B.; Cao, J.; Michino, M.; Luedtke, R. R.; Javitch, J. A.; Shi, L. Molecular determinants of selectivity and efficacy at the dopamine D3 receptor. *J. Med. Chem.* **2012**, *55*, 6689−6699.
(27) Capuano, B.; Crosby, I. T.; Lloyd, E. J.; Podloucka, A.; Taylor, D. A. Synthesis and preliminary pharmacological evaluation of 4′-arylalkyl analogues of clozapine. IV. The effects of aromaticity and isosteric replacement. *Aust. J. Chem.* **2008**, *61*, 930−940.
(28) Abdel-Fattah, M. A. O.; Lehmann, J.; Abadi, A. H. An interactive SAR approach to discover novel hybrid thieno probes as ligands for D2-like receptors with affinities in the subnanomolar range. *Chem. Biodiversity* **2013**, *10*, 2247−2266.
(29) Kenakin, T.; Watson, C.; Muniz-Medina, V.; Christopoulos, A.; Novick, S. A simple method for quantifying functional selectivity and agonist bias. *ACS Chem. Neurosci.* **2011**, *3*, 193−203.
(30) Vangveravong, S.; Zhang, Z.; Taylor, M.; Bearden, M.; Xu, J.; Cui, J.; Wang, W.; Luedtke, R. R.; Mach, R. H. Synthesis and characterization of selective dopamine D2 receptor ligands using aripiprazole as the lead compound. *Bioorg. Med. Chem.* **2011**, *19*, 3502−3511.
(31) Tschammer, N.; Elsner, J.; Goetz, A.; Ehrlich, K.; Schuster, S.; Ruberg, M.; Kühhorn, J.; Thompson, D.; Whistler, J.; Hübner, H.; Gmeiner, P. Highly potent 5-aminotetrahydropyrazolopyridines: enantioselective dopamine D3 receptor binding, functional selectivity, and analysis of receptor−ligand interactions. *J. Med. Chem.* **2011**, *54*, 2477−2491.
(32) Black, J. W.; Leff, P. Operational models of pharmacological agonism. *Proc. R. Soc. London, Ser. B* **1983**, *220*, 141−162.
(33) van der Westhuizen, E. T.; Breton, B.; Christopoulos, A.; Bouvier, M. Quantification of ligand bias for clinically relevant β2-adrenergic receptor ligands: implications for drug taxonomy. *Mol. Pharmacol.* **2014**, *85*, 492−509.